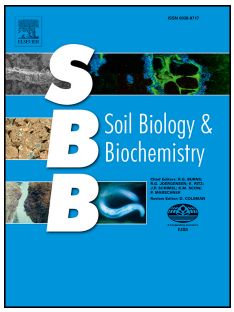

Initial soil formation by biocrusts: Nitrogen demand and clay protection control microbial necromass accrual and recycling

Baorong Wang, Yimei Huang, Na Li, Hongjia Yao, Env Yang, Andrey V. Soromotin, Yakov Kuzyakov, Vladimir Cheptsov, Yang Yang, Shaoshan An

PII: S0038-0717(22)00064-5

DOI: https://doi.org/10.1016/j.soilbio.2022.108607

Reference: SBB 108607

To appear in: *Soil Biology and Biochemistry*

Received Date: 23 August 2021

Revised Date: 6 February 2022

Accepted Date: 12 February 2022

Please cite this article as: Wang, B., Huang, Y., Li, N., Yao, H., Yang, E., Soromotin, A.V., Kuzyakov, Y., Cheptsov, V., Yang, Y., An, S., Initial soil formation by biocrusts: Nitrogen demand and clay protection control microbial necromass accrual and recycling, *Soil Biology and Biochemistry* (2022), doi: https://doi.org/10.1016/j.soilbio.2022.108607.

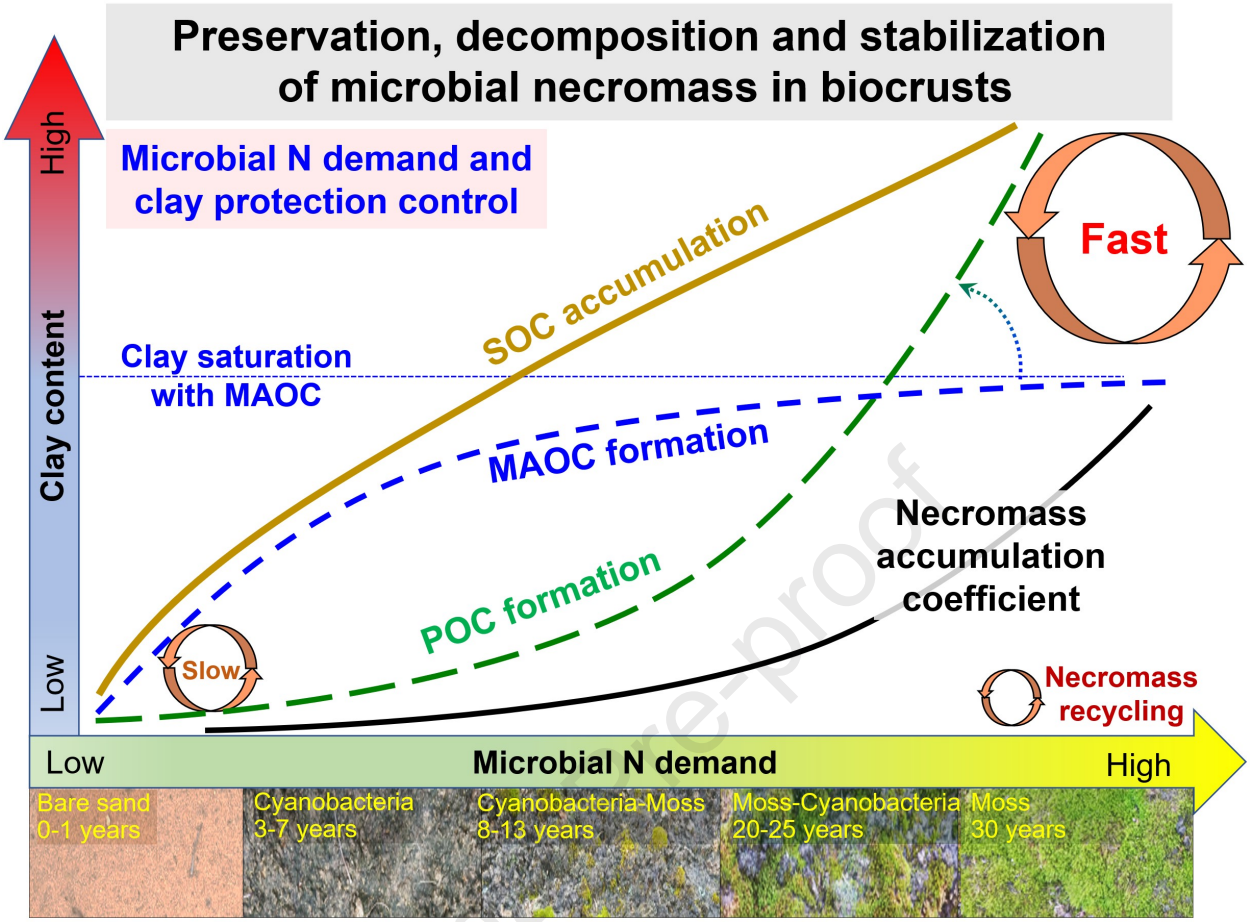

Initial soil formation by biocrusts: nitrogen demand and clay protection control microbial necromass accrual and recycling

Baorong Wang[1,2], Yimei Huang[3], Na Li[4], Hongjia Yao[4], Env Yang[4], Andrey V. Soromotin[5], Yakov Kuzyakov[6,7], Vladimir Cheptsov[8], Yang Yang[9], Shaoshan An [1, 4]*

Baorong Wang: wangbaorong92@163.com; Yimei Huang: ymhuang1971@nwsuaf.edu.cn; Na Li: 1356816040@qq.com; Hongjia Yao: 963904270@qq.com; Env Yang: 2215003782@qq.com; Andrey V. Soromotin: asoromotin@mail.ru; Yakov Kuzyakov: kuzyakov@gwdg.de; Vladimir Cheptsov: cheptcov.vladimir@gmail.com; Yang Yang: yangyang@ieecas.cn; Shaoshan An: shan@ms.iswc.ac.cn

[1] State Key Laboratory of Soil Erosion and Dryland Farming on the Loess Plateau, Institute of Soil and Water Conservation, Chinese Academy of Science and Ministry of Water Resources, Yangling 712100, China

[2] University of Chinese Academy of Sciences, Beijing 100049, China

[3] Key Laboratory of Plant Nutrition and the Agro-environment in Northwest China, Ministry of Agriculture, College of Natural Resources and Environment, Northwest A&F University, Yangling 712100 Shaanxi, China

[4] *State Key Laboratory of Soil Erosion and Dryland Farming on the Loess Plateau, Institute of Soil and Water Conservation, Northwest A&F University, Yangling 712100, China*

[5] *Institute of Environmental and Agricultural Biology (X-BIO), Tyumen State University, 6 Volodarskogo Street, Tyumen, Russia*

[6] *Department of Agricultural Soil Science, Department of Soil Science of Temperate Ecosystems, University of Gottingen, 37077, Goettingen, Germany*

[7] *Agro-Technological Institute, RUDN University, 117198 Moscow, Russia*

[8] *Soil Science Faculty, Lomonosov Moscow State University, 119991 Moscow, Russia*

[9] *State Key Laboratory of Loess and Quaternary Geology, Institute of Earth Environment, Chinese Academy of Sciences, Xi'an 710061, China*

*Corresponding author: Shaoshan An

E-mail address: shan@ms.iswc.ac.cn

Tel: +86 29 87012871; Fax: +86 29 87012210.

Address: No.26, Rd. Xinong, Yangling, Shaanxi, China. 712100

Declaration of competing interest

The authors declare that they have no known competing financial interests or personal relationships that could have influenced the work reported in this paper.

Abstract

Microbial biomass is increasingly considered to be the main source of organic carbon (C) sequestration in soils. Quantitative information on the contribution of microbial necromass to soil organic carbon (SOC) formation and the factors driving necromass accumulation, decomposition and stabilization during the initial soil formation in biological crusts (biocrusts) remains unavailable. To address this knowledge gap, we investigated the composition of microbial necromass and its contributions to SOC sequestration in a biocrust formation sequence consisting of five stages: bare sand, cyanobacteria stage, cyanobacteria-moss stage, moss-cyanobacteria stage, and moss stage on sandy parent material on the Loess Plateau. The fungal and bacterial necromass C content was analyzed based on the cell wall biomarker amino sugars. Microbial necromass was an important source of SOC, and was incorporated into the particulate and mineral-associated organic C (MAOC). Because bacteria have smaller and thinner cell wall fragments as well as more proteins than fungi, bacterial necromass mainly contributed to the MAOC pool, while fungal residues remained more abundant in the particulate organic C (POC). MAOC did not always increase with microbial necromass and POC more rapid accumulation than MAOC during initial soil formation suggests that the clay content was the limiting factor for stable C accumulation in this sandy soil. The necromass exceeding the MAOC stabilization level was stored in the labile POC pool (especially necromass from fungi). Activities of four enzymes (i.e., β-1,4-glucosidase, β-1,4-N-acetyl-glucosaminidase, leucine aminopeptidase, and alkaline phosphatase) increased with fungal and bacterial necromass, suggesting that the increasing activity of living microorganisms associated

with accelerated turnover and formation of necromass. Microbial N limitation raised the production of N acquisition enzymes (e.g., β-1,4-N-acetyl-glucosaminidase and leucine aminopeptidase) to break down necromass compounds, leading to further increase of the nutrient pool in soil solution. The decrease of microbial N limitation along the biocrusts formation chronosequence is an important factor for the necromass accumulation during initial soil development. High microbial N demands and insufficient clay protection lead to fast necromass reutilization by microorganisms and thus, result in a low necromass accumulation coefficient, that is, the ratio of microbial necromass to living microbial biomass (on average, 9.6). Consequently, microbial necromass contribution to SOC during initial soil formation by biocrust is lower (12-25%) than in fully developed soil (33%-60%, literature data). Nitrogen (N) limitation of microorganisms and an increased ratio between N-acquiring enzyme activity and microbial N, as well as limited clay protection, resulted in a low contribution of microbial necromass to SOC by initial formation of biocrust-covered sandy soil. Summarizing, soil development leads not only to SOC accumulation, but also to increased contribution of microbial necromass to SOC, whereas the plant biomass contribution decreases.

Keywords: *extracellular enzyme activities; particulate organic carbon; mineral-associated organic matter; initial soil formation; carbon sequestration; microbial residues*

1. Introduction

Biological soil crusts (hereafter referred to as "biocrusts") cover approximately 12% of Earth's terrestrial surface (Rodriguez-Caballero et al., 2018). Biocrusts are composed of photoautotrophic communities such as cyanobacteria, chlorophyte algae, lichens and mosses and co-occur with heterotrophic bacteria, fungi, and archaea (Belnap et al., 2008; Johnson et al., 2012; Pointing and Belnap, 2012). From the initial CO_2 fixation by microorganisms (Liu et al., 2018) to the later increase of soil organic carbon (SOC) content by inputs from simple vascular plants (i.e., mosses, Liu et al., 2018), biocrusts accelerate C and nutrient biogeochemical cycling in arid and semiarid regions (Grote et al., 2010; Duran et al., 2021) as well as in cold environments. For example, a global meta-analysis suggested that the SOC content under biocrusts generally increased by 71% compared to soil without crust cover (Xu et al., 2022). Biocrusts-derived organic C consists mainly of carbohydrate-C and free fatty acids (Dümig et al., 2014; Baumann et al., 2021). The high content of carbohydrate-C in well-developed biocrusts (e.g., mosses) is responsible for the high water solubility of organic C, increasing downward movement and thus induces initial soil formation (Dümig et al., 2014; Koester et al., 2021).

Microorganisms in soil biocrusts mediate C cycling processes by fixing atmospheric CO_2 (Duran et al., 2021) and degrading microbial, algae, lichen and moss residues (Pointing and Belnap, 2012). After microbial death and subsequent lysis and fragmentation, cell wall compounds contribute to the necromass pool and further to SOC sequestration (Miltner et al., 2012; Liang et al., 2017; Liang, 2020). Emerging

evidence reveals that microbial necromass contributes more than 50% of the SOC sequestration in developed soils (Huang et al., 2019; Liang et al., 2019; Wang et al, 2021a). However, the contribution of microbial necromass to SOC accumulation during initial soil formation in biocrust-dominated surfaces remains completely unclear.

The balance between mineralization and stabilization of organic matter influences the formation and decomposition of microbial necromass and its contribution to SOC accumulation (Cui et al., 2020; Liang et al., 2020; Čapek et al., 2021). Microbial necromass can bind to clay minerals and thus majorly forms mineral-associated organic C or becomes microaggregates stabilized in the soil (Ye et al., 2019; Buckeridge et al., 2020; Possinger et al., 2020; Yang et al., 2021). However, this physically-protected necromass can be enzymatically broken down into fragments that are released into soil solution and can be used by living microorganisms (Li et al., 2019; Yang et al., 2021). This is mainly because microbial necromass is an optimal substrate with high contents of N and P, that can be exploited by microorganisms to meet their C (energy) and nutrient requirements (Buckeridge et al., 2020; Cui et al., 2020).

Microbial necromass accumulation and decomposition are largely controlled by stoichiometric imbalances between microbial communities and their resources (Zechmeister-Boltenstern et al., 2015; Liang et al., 2020). The recycling of nutrients derived from dying microbial biomass or its residues is an important mechanism, by which microorganisms meet their nutrient requirements (López-Mondéjar et al., 2018;

Buckeridge et al., 2020; Čapek et al., 2021). The active part of the microbial community instantly recycles N from the decaying part of the community, when the available N forms are insufficient (Cui et al., 2020; Čapek et al., 2021). Microbial necromass reutilization is a more efficient strategy than obtaining N from non-readily decomposable soil organic matter (SOM) or alleviating N deficiency under labile C excess (Cui et al., 2020). Various extracellular enzymes, such as chitinases, decompose amino sugar polymers as an alternative N source for microorganisms when readily available N is limited (Li et al., 2019).

Environmental conditions and microbial nutrient demands have a strong influence on necromass recycling (Chen et al., 2019; Buckeridge et al., 2020; López-Mondéjar et al., 2020; Čapek et al., 2021). For example, high N availability accelerates microbial necromass accumulation (Ding et al., 2010; Fan et al., 2020), but only if available C is sufficient for growth (Chen et al., 2020). A nutrient-rich environment stimulates microbial growth with high biomass yield and necromass accumulation (Shao et al., 2021). Low precipitation increases microbial necromass recycling efficiency mainly because it limits nutrients and water availability, and especially drying-rewetting cycles especially contribute to the formation of mineral -associated SOM (Shahbaz et al., 2017; Buckeridge et al., 2020; Zhang et al., 2021). Thus, nutrient deficiencies or environmental constraints stimulate the microbial degradation of necromass by extracellular enzymes (e.g., β-1,4-N-acetyl-glucosaminidase, leucine aminopeptidase, Li et al., 2019; Donhauser et al., 2020). This is mainly because microbial necromass has high N and P contents,

154 and consists of proteins, fungal chitin, glycoproteins, nucleic acids and bacterial
155 peptidoglycans, whose hydrolysis greatly contributes to the formation of a
156 bioavailable dissolved organic N and P pool (Hu et al., 2017, 2020; Warren, 2021).
157 Additionally, rapid abiotic retention of microbial necromass by adsorption to soil
158 mineral particles (e.g., by drying-rewetting cycles) and localization in micro- and
159 nanopores increases the SOC stock (Kravchenko et al., 2019; Buckeridge et al.,
160 2020;). Consequently, a low clay content increases microbial necromass
161 decomposition (Hu et al., 2020). Therefore, the microbial demand for C and N,
162 environmental C and N availability, and clay protection are the major factors that
163 determine the accumulation and decomposition of necromass. This is especially
164 crucial during initial soil formation because of low clay and organic matter contents,
165 and a consequently strongly limited possibility for biochemical protection and
166 encapsulation in the pores of microaggregates. Biocrusts play a crucial role during the
167 initial stages of soil formation and organic matter accumulation. However,
168 biocrust-dominated soils are strongly limited by low moisture and nutrients (Johnson
169 et al., 2012) and consequently by the formation and accumulation of microbial
170 residues; thus, organic matter differs from that in already developed soils.

171 To clarify microbial necromass composition and its contribution to SOC
172 accumulation, we investigated the biocrust formation chronosequence: bare sand,
173 cyanobacteria, cyanobacteria-moss, moss-cyanobacteria, and moss. This is a typical
174 sequence on the same soil, consisting of five stages that may take approximately 30
175 years in the semi-arid climate. Fungal and bacterial necromass was calculated based

on the microbial markers: glucosamine and muramic acid. Soil and environmental factors affecting microbial necromass formation and its contributions to SOC sequestration were explored based on the activities of extracellular enzymes, available nutrients, and organic C pools. We addressed the following questions: (1) How does microbial necromass, including fungal and bacterial necromass, contribute to SOC accumulation during initial soil formation in the biocrust formation chronosequence? (2) What are the effects of extracellular enzymes, available nutrients, particulate and mineral-associated organic C on microbial necromass accumulation? (3) Which soil properties are the most critical determinants of microbial necromass accumulation and decomposition (based on the microbial nutrient limitation and their necromass content)? Based on these questions, we developed the three hypotheses: (1) The richness of higher plant species stimulates microbial growth and biomass accumulation by increasing belowground C allocation (roots and rhizodeposition), leading to increased necromass formation and SOC accumulation (Prommer et al., 2019; Cotrufo et al., 2019; Sokol and Bradford, 2018). We hypothesized that the microbial necromass content and its contribution to SOC increase with the biocrust formation chronosequence. (2) As nutrient availability importantly determines microbial necromass accumulation (Shao et al., 2021; Wang et al., 2021b), their association with mineral particles to form MAOC contributes to stable SOC (Yang et al., 2021). We hypothesized that increased soluble nutrients during biocrusts formation facilitate live microbial populations and hence necromass formation, which contributes to increased SOC mainly in the form of MAOC. (3) As the stoichiometric

198 ratio of nutrients controls the necromass accumulation and its contribution to SOC
199 (Čapek et al., 2021; Cui et al., 2020; Deng and Liang, 2021), and clay protection is the
200 main mechanism for necromass medium- and long-term stabilization (Buckeridge et
201 al., 2020; Hu et al., 2020). Thus, we hypothesize that extracellular enzymes released
202 by microorganisms for nutrient mining and the clay content regulate the microbial
203 necromass recycling and accumulation during initial soil formation.

204

205 ## 2. Material and methods

206 ### *2.1 Site description and experimental design*

207 The field experiment was performed in Liudaogou, Shenmu (northern Loess
208 Plateau), Shaanxi Province, China (38°46′–38°51′ N, 110°21′–110°23′). It is the
209 center of the "wind-water erosion staggered area" of the Loess Plateau. This area has a
210 semiarid climate, where the mean annual precipitation is 409 mm, and the potential
211 evapotranspiration is 1337 mm. The mean annual temperature of the sites is 8.4 °C,
212 and the elevation is between 1,081 and 1,274 m. Biocrusts comprised of
213 cyanobacteria and moss-dominated crust are widely distributed in this region. The soil
214 clay content (< 0.002 mm) of cyanobacteria, cyanobacteria-moss, moss-cyanobacteria,
215 and moss in the BSC horizons and 0–2 cm soil layer is shown in Table 1. The soil was
216 classified as an arenosol according to the World Reference Base for Soil Resources
217 (IUSS Working Group WRB, 2015).

All sites have a similar orientation and inclination. Bare sand (~ 0–1 years old) and four biocrust formation stages, namely, cyanobacteria (~ 3–7 years old), cyanobacteria-moss (~ 8–13 years old), moss-cyanobacteria (~ 20–25 years old), and moss (~ 30 years old), were evaluated. Cyanobacteria-moss and moss-cyanobacteria stages refer to cyanobacteria-dominated biocrusts (coverage of cyanobacteria > 80% and moss < 20%) and moss-dominated biocrusts (coverage of moss > 80% and cyanobacteria < 20%), respectively. The biocrust coverage was measured with a point-intercept method using a 25 cm × 25 cm gridded square (Belnap et al., 2001). For the soil sample collection (August 2018), we randomly selected 5 representative sites: 40 m × 40 m squares in each site with a distance over 100 m between any two sites. In each 40 × 40 m plot, an "S"-shaped random-sampling strategy with 12–15 small sampling locations was chosen. The soil samples from the 12–15 sampling points in each plot were mixed to obtain a representative sample of approximately 2 kg. Forty-five representative samples (4 stages × 5 replicates = 20 samples for the biocrust (BSC) horizon and 5 stages × 5 replicates = 25 samples for the 0–2 cm soil layer) including the BSC horizon and the 0–2 cm mineral soil layer underlying the biocrusts (Gao et al., 2017), were collected. The BSC horizon refers to the biological soil crust horizon, which consists of a colloidal complex of cryptogamic plants and associated soil microscopic organisms with surface soil particles. The measured biocrust thicknesses of cyanobacteria, cyanobacteria-moss, moss-cyanobacteria, and moss were approximately 7.2±2.2 mm, 9.6±1.9 mm, 11.1±1.9 mm, and 10.9±1.8 mm, respectively. After careful and thorough removal of moss tissues and residues from

240 the soil, the collected samples were put into a foam box with an ice pack and moved
241 to a 4 °C refrigerator within 24 h. Soil samples were separated into two parts: one part
242 was immediately analyzed for microbial biomass and extracellular enzyme activities
243 within one week. Another part of the air-dried sample was passed through a 2 mm
244 sieve for particle size and mineral-associated organic C determination. A part of the
245 soil sample was passed through the 0.15 mm size and tested for basic chemical
246 properties and amino sugar analysis.

247

248 ***2.2 Analysis***

249 The soil organic carbon (SOC) content was determined by dichromate oxidation
250 (Walkley and Black, 1934). Soil total nitrogen (N) and total phosphorus (P) contents
251 were measured using the Kjeldahl method and vanadium molybdate yellow
252 colorimetric method, respectively. The soil microbial biomass contents of C, N, and P
253 (MBC, MBN, and MBP) were measured using the chloroform-fumigation-extraction
254 method according to Brookes et al. (1982, 1985) and Vance et al. (1987). Briefly, two
255 sample parts were subjected to fumigation with $CHCl_3$ for 24 h at 25 °C, and two
256 others were not subjected to fumigation. The fumigated and nonfumigated soil
257 samples were extracted in 50 ml 0.5 M K_2SO_4 at a ratio of 1:4 (W/V) for microbial
258 biomass C and N and 50 ml 0.5 M $NaHCO_3$ at a ratio of 1:20 (W/V) for P. The
259 microbial biomass C, N and P contents were calculated according to the difference
260 between fumigated and nonfumigated samples and were adjusted using the

261 experimentally derived conversion factor E, where Ec, Ec and Ep = 0.45, 0.45 and
262 0.40, respectively (Fanin et al., 2013; Wu et al., 1990). The dissolved organic C, N
263 and inorganic P (DC, DN, and DP) contents were calculated from the unfumigated
264 samples (Chen et al., 2018; Hamel et al., 2006; Li et al., 2015).

265 Particulate organic C and mineral-associated organic C fractions were
266 determined according to the method of Sokol et al. (2019) and Sokol and Bradford.
267 (2018). In brief, soil samples (20 g air-dried soil) were shaken with 60 ml of the
268 chemical dispersant sodium hexametaphosphate for 18 h and then thoroughly rinsed
269 through a 0.053 mm sieve to separate the POC fraction (> 0.053 mm) and the MAOC
270 fraction (< 0.053 mm). The collected fractions were dried at 65 °C and then crushed
271 to 0.15 mm size for SOC determination.

272 The activities of four common hydrolytic enzymes associated with the microbial
273 acquisition of C, N, and P from organic residues (including β-1,4-glucosidase (BG),
274 β-1,4-N-acetyl-glucosaminidase (NAG), leucine aminopeptidase (LAP), and alkaline
275 phosphatase (AP)) were measured in 96-well plates with appropriate fluorescently
276 linked substrates and analyzed on a microplate fluorometer (DeForest and Moorhead,
277 2020; Li et al., 2019).

278 Amino sugar (e.g., glucosamine, galactosamine, mannosamine, and muramic
279 acid) contents were determined according to the method of Zhang & Amelung (1996).
280 Briefly, approximately 0.3 mg of N soil samples and standard soil samples (in which
281 the amino sugar content is known (measured many times), used for calibration) were
282 hydrolyzed for 8 h at 105 °C using 10 ml of 6 M HCl. After cooling, 100 μl internal

standard 1-inositol (1 mg/ml) was added. Then, the sample was filtered through Whatman qualitative circles (12.5 cm diameter), and the filtrate was dried completely by a rotary evaporator and redissolved in deionized water. The pH of the samples was adjusted to 6.6–6.8, and the samples were centrifuged and freeze-dried. Then, methanol was added to the freeze-dried residue and subsequently centrifuged to extract the amino sugars from the residues. The extracted amino sugar was dissolved in 1 ml deionized water, and then 100 μl of the internal standard N-methyl-D-glucamine (1 mg/ml) was added. A standard series of amino sugars was also established. Muramic acid was first dried under N_2 at 45 °C and then added to glucosamine, galactosamine, mannosamine, myo-inositol, N-methyl-D-glucamine, and 1 ml of deionized water, in that order. The purified samples and standard series of amino sugars were reacted with hydroxylamine hydrochloride and 4-(dimethylamino) pyridine for 30 min at 75–80 °C, and the vial was shaken 4–5 times during the heating process using a vortex instrument. The vial was cooled to room temperature, 1 ml of acetic anhydride was added, the reaction was allowed to proceed at 75–80 °C for 1 hour; the vial was shaken 5–6 times during the heating process using a vortex instrument. The vial was closed, and the recovered amino sugars were transformed into aldononitrile derivatives, which were extracted with 1.5 mL of dichloromethane from the aqueous solution. Excess anhydride was removed with 1 mol L^{-1} HCl and deionized water. The final organic phase was dried with N_2 at 45 °C and dissolved in 200 μL of ethyl acetate-hexane (1:l). The amino sugar derivatives were separated on a gas chromatograph (GC-2014C, Shimadzu, Japan) equipped with a DB-5 column (60

m × 0.25 mm × 0.25 μm). Fungal and bacterial necromass were calculated based on equations (1) and (2), according to Liang et al. (2019).

Fungal necromass C = (glucosamine /179.17 – 2 ×muramic acid /251.23) × 179.17 × 9 (1)

Bacterial necromass C = muramic acid × 45 (2)

The coefficients 179.17 and 251.23 in equation (1) are the molecular weights of glucosamine and muramic acid, respectively; 9 is the conversion value of fungal glucosamine to fungal necromass C; and 45 is the conversion value from muramic acid to bacterial necromass C (Appuhn and Joergensen, 2006; Joergensen, 2018). The total microbial necromass C (MNC) was estimated as the sum of fungal-derived C (FNC) and bacterial-derived C (BNC). The proportion of total microbial necromass C in SOC represents the microbial necromass contribution to SOC sequestration (Liang et al., 2019).

2.3 Statistical analysis

One-way ANOVA followed by the post hoc Tukey HSD test ($\alpha = 0.05$) was carried out with IBM SPSS Statistics 21 (SPSS, Chicago, Illinois USA) software to test the significant differences in soil chemical properties, microbial biomass, extracellular enzyme activities, available nutrients, POC, MAOC, microbial necromass C and amino sugars in the biocrust formation stages. Regression analysis was performed using IBM SPSS Statistics 20 software to assess the relationships

between SOC, POC and MAOC and fungal, bacterial, and microbial necromass C. To explore the clay saturation with MAOC, regression analysis was performed to assess the relationships between SOC, clay contents, POC, MAOC, POC/MAOC and fungal and bacterial necromass C. The regressions were considered significant at a level of $p < 0.05$. Redundancy analysis (RDA) was performed to explore the relationships among microbial biomass, extracellular enzymes, available nutrients, POC and MAOC (explanatory variables), microbial necromass and amino sugars (response variables). Prior to analysis, detrended correspondence analysis (DCA) was used to select the appropriate response model for the subsequent direct gradient analyses. The length of the first DCA ordination axis was < 3 for the necromass and amino sugar dataset, which indicated a linear response along the axis. Forward selection in this model was used to determine the most significant factors that influenced amino sugars and microbial necromass C. The variables were incorporated stepwise into the model according to their increasing effect on the variance and their significance tested by the Monte Carlo permutation test (Legendre and Legendre, 2012).

Stoichiometric analysis of soil enzyme activities was used to identify potential C, N and P limitations in the soil. The enzymatic stoichiometric vector characteristics (including vector length and vector angle) were calculated according to Moorhead et al. (2016). These values were used as a rough reflection of microbial nutrient limitation: High vector length implies microbial C limitation, whereas a vector angle lower than 45° indicates N limitation; otherwise, P limitation dominates (Bai et al., 2021). By using 1.0 as a horizontal and vertical baseline along the axis of enzyme

activity ratios (NAG+LAP/AP as x-axis and BG/NAG+LAP as y-axis), four groups of microbial resource limitations (N limitation, P limitation, C and N colimitation and C and P colimitation) were categorized (Bai et al., 2021; Cui et al., 2020). The vector length and vector angle are calculated following Equations (1) and (2):

Vector length=$\sqrt{(\ln(BG)/ln(NAG+LAP))^2+(\ln(BG)/\ln(AP))^2}$ (1)

Vector angle = DEGREES{ATAN2[(ln(BG) / ln(AP), (ln(BG) / ln(NAG+LAP)]} (2)

The necromass accumulation coefficient (NAC) was calculated using Equation (3) Zhang et al. (2021).

$$NAC = \frac{C_{Necromass}}{C_{living\ \ Biomass}} \qquad \text{Equation (3)}$$

To test the strength of microbial homeostasis in biocrust-covered sandy soil, we calculated the degree of stoichiometric homeostasis for microorganisms using the 1/H coefficient (Equation (4)). The 1/H coefficient is the slope of the regression between log (resource ratio; C/N in bulk soil, dissolved matter and enzyme) and log (biomass ratio; microbial C/N ratio) and should equal a value between zero and one (Makino et al., 2003; Persson et al., 2010):

$$\log(y) = \frac{1}{H}\log(x) + \log(c) \qquad \text{Equation (4)}$$

where x is the resource C/N stoichiometry, y is the microorganisms' C/N stoichiometry, and c is a constant. If the regression relationship was nonsignificant ($p > 0.05$), 1/H was set to zero, and the microorganisms were considered "strictly homeostatic." All datasets with significant regressions and $0 < 1/H < 1$ were arbitrarily classified as follows: $0 < 1/H < 0.25$ "homeostatic", $0.25 < 1/H < 0.5$ "weakly homeostatic", $0.5 < 1/H < 0.75$ "weakly plastic", and $1/H > 0.75$ "plastic"

370 (Persson et al., 2010).

371

372 ## 3. Results

373 ### *3.1 Microbial necromass and its contribution to organic C accumulation*

374 Initial soil formation by biocrusts increased the fungal and bacterial necromass
375 contents in the 0–2 cm soil layer compared to bare sand (Fig. 1a-b, $p < 0.05$).
376 Although SOC and microbial biomass increased from the cyanobacteria to moss stage
377 (Table 1, $p < 0.05$), there were no differences in the fungal necromass contents
378 between formation stages in the BSC horizon (Fig. 1a, $p > 0.05$). Except for the bare
379 sand, bacterial necromass contents remained constant in the BSC horizon but
380 decreased in the 0–2 cm mineral soil from the cyanobacteria stage to the moss stage
381 (Fig. 1b). Other microbial cell molecules, such as galactosamine and mannosamine
382 contents, remained stable over the course of biocrust formation (Table 1). The
383 microbial necromass C contribution to SOC ranged from 12% (in bare sand) to 25%
384 in various biocrust stages (Fig. 1c). The fungal:bacterial necromass ratio at 0–2 cm
385 increased from the cyanobacteria to the moss stage, indicating that larger fungal
386 necromass contributed to increased SOC (Fig. 1d, $p < 0.05$).

387 The contribution of bacterial necromass C to SOC ranged from 2.6% (in bare
388 sand) to ~ 7.7%, while the contribution of fungi at various biocrust stages ranged from
389 10% (bare sand) to 21% (Fig. 1e-f). Fungal necromass (> 67% of the total necromass)
390 consistently contributed more to SOC than did bacterial necromass C (Fig. 1g). The

391 contribution of bacterial necromass C to SOC and microbial necromass in the BSC
392 horizon was higher than that in the 0–2 cm soil layer, indicating that bacteria
393 contributed more to SOC formation in the BSC than in the underlying soil (Fig. 1e).
394 The ratio of microbial necromass C/microbial biomass C (necromass accumulation
395 per unit of microbial biomass C: necromass accumulation coefficient) decreased from
396 the cyanobacteria stage to the moss stage (Fig. 1h, $p < 0.05$). The necromass
397 accumulation coefficient increased from the BSC horizon to the mineral soil (0–2 cm).
398 This suggests relatively higher necromass stabilization and preservation in 0–2 cm
399 mineral soil (Fig. 1h).

400

401 ***3.2 Extracellular enzymes and microbial nutrient limitation***

402 The enzyme activities of NAG and AP in both layers and LAP in the 0–2 cm
403 layer increased from bare sand to the moss stage (Fig. 2b-d, $p < 0.05$). The
404 C-acquiring enzyme (BG) activity /microbial biomass C ratio (specific enzyme
405 activity per microbial biomass unit: microbial enzyme activity coefficient) increased
406 from the BSC horizon to the 0–2 cm layer, suggesting higher microbial C demands in
407 the subsurface layer of biocrust-covered sandy soil (Fig. 2e). The N-acquiring enzyme
408 (NAG+LAP) activity/microbial biomass N ratio increased from cyanobacteria to moss
409 in the BSC horizon, suggesting higher microbial N demands with biocrust formation
410 sequences (Fig. 2f).

411 The decreasing vector length of the enzyme ratio in the 0–2 cm soil depth from
412 the bare sand to moss stage suggests a decrease in C limitation for microorganisms
413 with biocrust formation (Fig. 3a). The vector angles of the enzyme ratio were always
414 less than 45° (Fig. 3b), indicating that microbial N limitation was common in all
415 biocrust stages but it tends to decrease due to the increase in N-acquisition enzymes
416 and their enzymatic coefficients with biocrust formation (Fig. 2e-f and Fig. 3b).
417 Microbial C and N colimitation and a higher C- and N-acquiring enzyme
418 activity/microbial biomass C and N ratio were found in bare sand (Figs. 2e, f and 3e,
419 f), suggesting that biocrust formation eliminates the microbial C limitation, whereas N
420 limitation remains (Fig. 3c-d). Consequently, stronger microbial nutrient limitation
421 leads to a higher recycling intensity of necromass, decreasing the contribution of
422 necromass to SOC.

423

424 ***3.3 Effects of biocrust formation and microbial necromass accumulation on soil***
425 ***organic matter fractions***

426 The POC and MAOC increased with SOC content (Fig. 4a, $p < 0.001$). The
427 fungal, bacterial, and total microbial necromass C increased with SOC content (Fig.
428 4b; $p < 0.001$), indicating the critical role of microbial necromass in SOC formation
429 in biocrust-dominated soil. Bacterial necromass was more strongly correlated with
430 MAOC, while fungal necromass was more strongly correlated with POC (Fig. 4c-d, p
431 < 0.001). Similarly, POC and MAOC increased with fungal, bacterial, and microbial

necromass C (Fig. 4c-d; $p < 0.001$). Microbial necromass was more correlated with POC than MAOC (Fig. 4a-b and Table 1) and MAOC did not always increase with necromass (Fig. 5a-b), suggesting that more necromass was stabilized by forming POC due to the low clay content (only 1–2%). The POC/MOAC ratio increased with SOC content (Fig. 5c), indicating that POC accumulated faster than MAOC. Microbial necromass C increased with clay and silt contents (excluding bacterial necromass C in the BSC horizon; Fig. 5d-e, $p < 0.01$), indicating that a higher clay and silt content could protect fungal and bacterial necromass and further benefit their accumulation.

3.4 Accumulation of microbial necromass depending on dissolved N content

Microbial necromass C increased with living biomass, enzyme activities and dissolved nutrients, indicating that a large living microbial biomass can stimulate necromass accumulation (Fig. S1a-i, $p < 0.001$). Dissolved N was the most important factor affecting microbial necromass accumulation in BSC horizon, while other soil properties (i.e., MBN, DN, MBC, DC, clay contents, LAP, and POC) explained microbial necromass stabilization at 0–2 cm (RDA results, Fig. 6 a-d, $p < 0.01$). The POC, but not MAOC, was an important factor influencing microbial necromass accumulation in the BSC horizon and 0–2 cm layer, suggesting that the POC plays an important role in necromass stabilization (Fig. 6 c-d, $p < 0.01$).

4. Discussion

4.1 Microbial necromass contents and their contribution to the SOC pool

Microbial necromass formation is determined by biomass production, death of microorganisms, and cell residue decomposition (Chen et al., 2021; Shao et al., 2021). Enzyme activities increase with living microbial biomass and necromass (Fig. S1). Consequently, rapid turnover of living microbial biomass produces more necromass. A greater amount of living biomass and faster microbial growth result in higher biomass production and further necromass accumulation, thereby contributing to SOC sequestration (Prommer et al., 2019; Chen et al., 2020). The microbial necromass to SOC ratio in the BSC horizon (from cyanobacteria (3–7 years old) to moss (~30 years old)) decreased, and the fungal:bacterial necromass ratio in the 0–2 cm soil layer increased (from bare sand to moss) with biocrust formation (Fig. 1). Consequently, the contribution of undecomposed moss residues to SOC accumulation increased, and thus fungal necromass especially accumulated (Fig. 1f). This is explained by the decomposition of complex organic matter (moss residues) that is dominated by fungi (López-Mondéjar et al., 2018; Algora Gallardo et al., 2021). Fungi are better adapted to degrade persistent plant biomass and organic matter, as well as hydrophobic substances, as they produce specific carbohydrate-active hydrolases (López-Mondéjar et al., 2020) and (per)oxidases (Xia et al., 2020; Deng et al., 2021). Bacteria contributed more to SOC formation in the surface (BSC horizon) than in the subsurface (0–2 cm mineral layer) of biocrust-dominated soil (Fig. 1e) because bacteria tend to recycle microbial necromass and insufficient clay protection in the

BSC horizon, thus accelerating the turnover of living and dead biomass (López-Mondéjar et al., 2018; López-Mondéjar et al., 2020);

Microbial necromass is an important organic matter source in biological crust-dominated sandy soil that contributes to SOC sequestration (Figs. 1 and 4) by incorporating into the POC and MAOC (Figs. 4 and 5). However, inconsistent with our first hypothesis, microbial necromass content and its contribution to SOC did not increase with the biocrust formation chronosequence (Fig. 1). The contributions of microbial necromass to SOC in the BSC horizon and 0–2 cm mineral soil layer range from 12% to 25%, much lower than their contributions to fully developed soils: > 50% in croplands and grasslands and ~ 35% in forests (reviewed by Khan et al., 2016; Liang et al., 2019; Huang et al., 2019). This phenomenon is mainly due to the (i) low nutrient content and availability of the initial soil formation may limit the microbial necromass accumulation compared to well-developed soils (Buckeridge et al., 2020; Shao et al., 2021; Wang et al, 2021); (ii) lower necromass accumulation coefficients show limiting microbial residue stabilization during the initial soil formation because of the very low clay content and poor microaggregation (Figs. 1 and 7). For instance, the necromass accumulation coefficient in biocrust-covered sandy soils of the Loess Plateau is 9.6 (Fig. 1), which is lower than those of the Qinghai-Tibet Plateau (16), Mongolian grassland soils (24), and other grasslands worldwide (30) (Zhang et al., 2021). Consequently, the contribution of microbial necromass to SOC increases in the following order: Loess Plateau biocrust-covered sandy soils (22%) < Qinghai-Tibet Plateau (33%) < Mongolian grassland (49%) < other grasslands worldwide (58%)(Fig.

497 1; Zhang et al., 2021). This increase corresponds to the progress of pedogenesis and
498 formation of secondary clay particles and water stable aggregates. The necromass
499 accumulation coefficient is regulated by biotic (microbial nutrient demands, etc.) and
500 abiotic (soil nutrient availability, clay content, etc.) factors (Buckeridge et al., 2020;
501 Zhang et al., 2021). The limited N content of sandy soils is mainly due to insufficient
502 inputs and the low diversity of N fixation pathways (Steven et al., 2012; Li et al.,
503 2020). Thus, the lower accumulation efficiency of microbial necromass C in our soil
504 is because of the sandy texture (low clay content, poor aggregation), which is related
505 to poor necromass preservation (Fig. 5) and/or high microbial N demands (Figs. 2 and
506 3)

507

508 ***4.2 Microbial necromass stabilization and preservation***

509 Microbial necromass contributes to SOC sequestration by forming particulate
510 and mineral-associated organic C (Figs. 4 and 5; Lavallee et al., 2019). The binding of
511 microbial necromass to soil particles is the main mechanism for their medium- and
512 long-term stabilization (Chen et al., 2020; Samson et al., 2020; Yang et al., 2021), in
513 which organo-mineral interfaces are dominated by N-enriched residues (Buckeridge et
514 al., 2020; Possinger et al., 2020). Although POC and MAOC increased with the
515 microbial necromass C contents, necromass was more closely correlated with POC
516 than with MAOC (Fig. 4). Unlike in developed soils, in which more necromass is
517 found in the MAOC pool (Lavallee et al., 2019; Samson et al., 2020), this result

518 suggests that more necromass is present in biocrust-dominated soils through POC
519 formation (Figs. 5 and 6). This is explained by (i) microbial necromass recycling or
520 destabilization decreasing its accumulation (Figs. 4 and 7); (ii) the accumulation of
521 MAOC may become saturation due to the limitation of clay and silt content (Fig. 5a;
522 Craig et al., 2021); (iii) formation of POC by part of the microbial necromass (e.g.,
523 fungal hyphae), which plays an important role in SOC accrual (Lavallee et al., 2019;
524 Samson et al., 2020); (iv) the retained thin soil water films in aggregates allowed
525 continued microbial recycling of necromass from the MOAC (Manzoni et al., 2012),
526 while the POC decomposition may be limited by low soil water because water-driven
527 microbial nutrient transformations in biocrusts (Maier et al., 2021). This result may
528 suggest that the bacterial necromass mainly contributed to the MAOC pool, while
529 fungi contributed more to POC (Fig. 4). This is possibly because (i) bacteria are
530 smaller and have thinner cell wall fragments compared to fungi (Schweigert et al.,
531 2015); (ii) bacteria inhabit biofilms and soil aggregate pores (Guhra; et al., 2021;
532 Yang et al., 2021), because the attachment of bacteria cells to mineral surfaces and
533 their active habitat formation increases the soil aggregation potentially reducing the
534 bacterial necromass decomposition (Krause et al., 2019).

535 In the BSC horizon, MAOC did not continuously increase with microbial
536 necromass, presumably due to saturation of MAOC, because of the limited amount of
537 clay and silt particles in biological crust dominated sandy soil (Fig. 5a; Matus, 2021).
538 Microbial necromass stabilization might be limited by the direct sorption of exudates
539 (e.g., released from moss, algae) outcompetes sorption of microbial residues on clay

or silt particles (Walker et al., 2003; Kubiak-Ossowska et al., 2017; Guhra; et al., 2021). Departure from our second hypothesis, the POC increased with microbial necromass (especially fungal necromass) and the POC/MAOC ratio increased with SOC, suggesting that the poor preservation conditions (e.g., limited clay content) leads to more necromass remaining as POC (Figs. 5 and 6). Microbial necromass decomposition is slow in soils with high clay content and formation of stable microaggregates (Hu et al., 2020) because adsorption on clays and protection in microaggregates are key factors controlling physico-chemical and physical stabilization (Doetterl et al., 2015). Indeed, microbial necromass-formed POC lack physico-chemical protection, which leads to their direct contact with living microorganisms and increases the likelihood of their degradation by exoenzymes (Kuzyakov and Mason-Jones, 2018; Lavallee et al., 2019). The living microbial biomass increases, but necromass remains stable, from the cyanobacteria to moss stage in BSC horizons (Fig. 1 and Table 1), suggesting a rapid necromass recycling because of the limited protection by clay or microaggregates as a result of low clay content during initial soil formation (Figs. 5 and 7). This phenomenon occurs mainly because POC generally has rapid turnover (Gunina and Kuzyakov, 2014; Poeplau et al., 2018), whereas the amounts of clay and silt particles (Fig. 5) limit necromass preservation, especially during initial soil formation (Lavallee et al., 2019).

4.3 Microbial necromass accumulation regulated by dissolved N

In line with our third hypothesis, extracellular enzyme stoichiometry revealed

562 that i) microbial N limitation is common in biological crust dominated sandy soil (Fig.
563 3), and ii) N-acquiring enzyme activities increased with biocrust formation,
564 accelerating necromass decomposition and alleviating microbial N limitation during
565 initial soil formation (Fig. 2). The release of extracellular enzymes by microorganisms
566 to mineralize organic compounds is an important mechanism to maintain homeostasis
567 of microbial C:N:P ratio and overcome nutrient limitations (Mooshammer et al., 2014;
568 Zechmeister-Boltenstern et al., 2015). Fungal and bacterial necromass increased with
569 the soil DC and DN levels (Fig. S1), suggesting that necromass decomposition greatly
570 contributes to the formation of a bioavailable nutrient pool. Microbial necromass is
571 richer in N than SOM is (Cotrufo et al., 2019; Liang et al., 2019), and therefore, N
572 mining from necromass is a more efficient strategy than N acquisition from
573 recalcitrant soil organic matter (Buckeridge et al., 2020; Cui et al., 2020). Microbial
574 demand for N leads to necromass mineralization when the available N forms are
575 insufficient (Cui et al., 2020; Čapek et al., 2021).

576 In view of microbial N limitation and increased N-acquiring (NAG+LAP)
577 enzyme activity/microbial biomass N ratio, as well as poor necromass preservation
578 (Figs. 2, 5 and 7), dissolved N is the most important factor influencing necromass
579 abundance in biocrust-covered sandy soils (Fig. 6). This is mainly because available
580 nutrients require less energy to use than bulk SOM (Liang et al., 2017), which
581 requires microorganisms to produce enzymes (Kaiser et al., 2014; Mooshammer et al.,
582 2014; Čapek et al., 2021). Under N-limited conditions, microorganisms synthesize
583 and release extracellular enzymes (e.g., NAG and LAP) to mobilize microbial

584 necromass for their N demand (Fig. 2). Consequently, N availability strongly affects
585 the accumulation or reutilization of microbial necromass during the initial formation
586 of biocrust-covered sandy soil. This is mainly because the homoeostatic growth of
587 microorganisms requires an appropriate ratio (e.g., microbial biomass C/N ratio
588 ranging from 2.4 to 4.3 in the BSC horizon and 0–2 cm soil layer) of nutrients (e.g., C,
589 N, and P) to maintain the stoichiometric balance that drives microbial metabolic
590 processes (Mooshammer et al., 2014; Liang et al., 2020). For example, the
591 homeostasis index (1/H) ranged from 0 to 0.24, indicating that the microbial C/N
592 stoichiometry in biocrust-covered sandy soil was homeostatic (Fig. S2). Microbial
593 community growth on various resources with extremely variable or low C/nutrient
594 ratios cannot be achieved solely via nonhomeostatic methods (Mooshammer et al.,
595 2014; Zechmeister-Boltenstern et al., 2015). Microorganisms require stoichiometric
596 homeostasis to maintain normal life activities by adjusting their own elemental
597 utilization efficiency or mobilizing resources by producing specific extracellular
598 enzymes (Mooshammer et al., 2014). Therefore, microorganisms maintain C/N
599 stoichiometric homeostasis by using bioavailable soluble substances or microbial
600 necromass (Kaiser et al., 2014; Chen et al., 2019) as well as nutrient recycling (Chen
601 et al., 2019; Bilyera et al., 2021). Potential shifts in microbial C/N stoichiometry and
602 dissolved organic C/N influence necromass accumulation (Fig. S3) because
603 stoichiometry controls nutrient mining from necromass (Cui et al., 2020; Čapek et al.,
604 2021).
605

5 Conclusions

Microbial biomass, extracellular enzymes, available nutrients, particulate and mineral particles determine the accumulation and recycling of necromass during initial soil formation. Microbial N limitation was common in all biocrust stages, but it decreased during biocrust development due to the increase in N-acquisition enzymes. MAOC did not always increase, but POC increased with microbial necromass, suggesting that the MAOC increase was limited by low clay content and consequently, led to stronger POC than MAOC accumulation in the BSC horizon. A potential explanation for the accumulation of POC relative to MAOC may also be that the retained thin soil water films in aggregates allowed necromass recycling from the MOAC, whereas POC decomposition might be limited by low soil water, but this needs further investigation in the future. Microbial N limitation and necromass destabilization (e.g., insufficient clay protection) lead to rapid necromass reutilization by microorganisms, resulting in a low necromass accumulation coefficient in biocrust-covered sandy soil. Microorganisms meet their nutrient demands by releasing extracellular enzymes to degrade necromass, and its decomposition forms a pool of dissolved nutrients. As a result, the microbial necromass C contributes to SOC in biocrust-covered sandy soil much lower than in fully developed soils. Consequently, the initial soil formation by biocrusts is characterized by strong N limitation and low clay content, leading to high activities of enzymes, especially of the N cycle, poor protection and stabilization of microbial necromass, leading to intensive reutilization and thus a low contribution of microbial residues to SOC sequestration.

Acknowledgments

This research was supported by the National Natural Science Foundation of China [41877074 and 42077072]. Vladimir Cheptsov (VC) was supported by the state assignment "Soil microbiomes: genomic diversity, functional activity, geography and biotechnological potential" (No. 121040800174-6). Yakov Kuzyakov (YK) thanks the support of the "RUDN University Strategic Academic Leadership Program". The publication was prepared with the support of the Tyumen Oblast Government project "TerrArctic" (West-Siberian Interregional Science and Education Center's project No. 89-DON) and project: Stability and Functions of Soil Carbon in Agroecosystems of Russia (CarboRus, 075-15-2021-610).

639 **References:**

640 Algora Gallardo, C., Baldrian, P., López-Mondéjar, R., 2021. Litter-inhabiting fungi
641 show high level of specialization towards biopolymers composing plant and
642 fungal biomass. Biology and Fertility of Soils 57, 77–88.

643 Appuhn, A., Joergensen, R.G., 2006. Microbial colonisation of roots as a function of
644 plant species. Soil Biology and Biochemistry 38, 1040–1051.

645 Bai, X., Dippold, M.A., An, S., Wang, B., Zhang, H., Loeppmann, S., 2021.
646 Extracellular enzyme activity and stoichiometry: The effect of soil microbial
647 element limitation during leaf litter decomposition. Ecological Indicators 121,
648 107200.

649 Baumann, K., Eckhardt, K.U., Acksel, A., Gros, P., Glaser, K., Gillespie, A.W.,
650 Karsten, U., Leinweber, P., 2021. Contribution of biological soil crusts to soil
651 organic matter composition and stability in temperate forests. Soil Biology and
652 Biochemistry 160, 108315.

653 Belnap, J., Phillips, S.L., Flint, S., Money, J., Caldwell, M., 2008. Global change and
654 biological soil crusts: Effects of ultraviolet augmentation under altered
655 precipitation regimes and nitrogen additions. Global Change Biology 14,
656 670-686.

657 Belnap, J., Rosentreter, R., Leonard, S., Kaltenecker, J., Williams, J., Eldridge, D.,
658 2001. Biological soil crusts: ecology and management. US Dept. of Interior TR.

659 Bilyera N., Dippold M.A., Blaicher J., Maranguit D., Kuzyakov Y. Blagodatskaya E.

2021. Microbial tradeoffs in internal and external use of resources regulated by P and C availability. European Journal of Soil Biology 106, 103353.

Brookes, P.C., Landman, A., Pruden, G., Jenkinson, D.S., 1985. Chloroform fumigation and the release of soil nitrogen: A rapid direct extraction method to measure microbial biomass nitrogen in soil. Soil Biology and Biochemistry 17, 837–842.

Brookes, P.C., Powlson, D.S., Jenkinson, D.S., 1982. Measurement of microbial biomass phosphorus in soil. Soil Biology and Biochemistry 14, 319-329.

Buckeridge, Kate M., La Rosa, A.F., Mason, K.E., Whitaker, J., McNamara, N.P., Grant, H.K., Ostle, N.J., 2020. Sticky dead microbes: Rapid abiotic retention of microbial necromass in soil. Soil Biology and Biochemistry 14, 107929.

Buckeridge, Kate M, Mason, K.E., Mcnamara, N.P., Ostle, N., Puissant, J., Goodall, T., Grif, R.I., Stott, A.W., Whitaker, J., 2020. Environmental and microbial controls on microbial necromass recycling, an important precursor for soil carbon stabilization. Communications Earth & Environment 1, 1–9.

Čapek, P., Choma, M., Tahovská, K., Kaňa, J., Kopáček, J., Šantrůčková, H., 2021. Coupling the resource stoichiometry and microbial biomass turnover to predict nutrient mineralization and immobilization in soil. Geoderma 385, 114884.

Chen, H., Zhao, X., Chen, X., Lin, Q., Li, G., 2018. Seasonal changes of soil microbial C, N, P and associated nutrient dynamics in a semiarid grassland of north China. Applied Soil Ecology 128, 89–97.

681 Chen, J., Ji, C., Fang, J., He, H., Zhu, B., 2020. Dynamics of microbial residues
682 control the responses of mineral-associated soil organic carbon to N addition in
683 two temperate forests. Science of the Total Environment 748, 141318.

684 Chen, J., Seven, J., Zilla, T., Dippold, M.A., Blagodatskaya, E., Kuzyakov, Y., 2019.
685 Microbial C:N:P stoichiometry and turnover depend on nutrients availability in
686 soil: A ^{14}C, ^{15}N and ^{33}P triple labelling study. Soil Biology and Biochemistry 131,
687 206–216.

688 Chen, X., Hu, Y., Xia, Y., Zheng, S., Ma, C., Rui, Y., He, H., Huang, D., Zhang, Z.,
689 Ge, T., Wu, J., Georg, G., Kuzyakov, Y., Su, Y., 2021. Contrasting pathways of
690 carbon sequestration in paddy and upland soils. Global Change Biology 27,
691 2478-2490.

692 Chen, X., Xia, Y., Rui, Y., Ning, Z., Hu, Y., Tang, H., He, H., Li, H., Kuzyakov, Y.,
693 Ge, T., Wu, J., Su, Y., 2020. Microbial carbon use efficiency, biomass turnover,
694 and necromass accumulation in paddy soil depending on fertilization.
695 Agriculture, Ecosystems and Environment 292, 106816.

696 Cotrufo, M.F., Ranalli, M.G., Haddix, M.L., Six, J., Lugato, E., 2019. Soil carbon
697 storage informed by particulate and mineral-associated organic matter. Nature
698 Geoscience 12, 989-994.

699 Craig, M.E., Mayes, M.A., Sulman, B.N., Walker, A.P., 2021. Biological mechanisms
700 may contribute to soil carbon saturation patterns. Global Change Biology 27,
701 2633-2644.

Cui, J., Zhu, Z., Xu, X., Liu, S., Jones, D.L., Kuzyakov, Y., Shibistova, O., Wu, J., Ge, T., 2020. Carbon and nitrogen recycling from microbial necromass to cope with C:N stoichiometric imbalance by priming. Soil Biology and Biochemistry 142, 107720.

Cui, Y., Wang, X., Zhang, X., Ju, W., Duan, C., Guo, X., Wang, Y., Fang, L., 2020. Soil moisture mediates microbial carbon and phosphorus metabolism during vegetation succession in a semiarid region. Soil Biology and Biochemistry 147, 107814.

DeForest, J.L., Moorhead, D.L., 2020. Effects of elevated pH and phosphorus fertilizer on soil C, N and P enzyme stoichiometry in an acidic mixed mesophytic deciduous forest. Soil Biology and Biochemistry 150, 107996.

Deng, S., Zheng, X., Chen, X., Zheng, S., He, X., Ge, T., Kuzyakov, Y., Wu, J., Su, Y., Hu, Y., 2021. Divergent mineralization of hydrophilic and hydrophobic organic substrates and their priming effect in soils depending on their preferential utilization by bacteria and fungi. Biology and Fertility of Soils 57, 65-76.

Deng; F, Liang, C., 2021. Revisiting the quantitative contribution of microbial necromass to soil carbon pool: Stoichiometric control by microbes and soil. Soil Biology and Biochemistry 164, 108486.

Ding, X., Zhang, X., He, H., Xie, H., 2010. Dynamics of soil amino sugar pools during decomposition processes of corn residues as affected by inorganic N

addition. Journal of Soils and Sediments 10, 758–766.

Doetterl, S., Stevens, A., Six, J., Merckx, R., Van Oost, K., Casanova Pinto, M., Casanova-Katny, A., Muñoz, C., Boudin, M., Zagal Venegas, E., Boeckx, P., 2015. Soil carbon storage controlled by interactions between geochemistry and climate. Nature Geoscience 8, 780-783.

Donhauser, J., Qi, W., Bergk- Pinto, B., Frey, B., 2020. High temperatures enhance the microbial genetic potential to recycle C and N from necromass in high-mountain soils. Global Change Biology 27, 1365-1386.

Dümig, A., Veste, M., Hagedorn, F., Fischer, T., Lange, P., Spröte, R., Kögel-Knabner, I., 2014. Organic matter from biological soil crusts induces the initial formation of sandy temperate soils. Catena 122, 196–208.

Duran P, de la Luz Mora M, Matus F, Barra PJ, Jofre I, Kuzyakov Y, Merino C 2021. Biological crusts to increase soil carbon sequestration: New challenges in a new environment. Biology 10, 1190.

Fan, Y., Yang, L., Zhong, X., Yang, Z., Lin, Y., Guo, J., Chen, G., Yang, Y., 2020. N addition increased microbial residual carbon by altering soil P availability and microbial composition in a subtropical Castanopsis forest. Geoderma 375, 114470.

Fanin, N., Fromin, N., Buatois, B., Hättenschwiler, S., 2013. An experimental test of the hypothesis of non-homeostatic consumer stoichiometry in a plant litter-microbe system. Ecology Letters 16, 764–772.

744 Gao, L., Bowker, M.A., Xu, M., Sun, H., Tuo, D., Zhao, Y., 2017. Biological soil
745 crusts decrease erodibility by modifying inherent soil properties on the Loess
746 Plateau, China. Soil Biology and Biochemistry 105, 49-58.

747 Grote, E.E., Belnap, J., Housman, D.C., Sparks, J.P., 2010. Carbon exchange in
748 biological soil crust communities under differential temperatures and soil water
749 contents: Implications for global change. Global Change Biology 16, 2763-2774.

750 Gunina, A., Kuzyakov, Y., 2014. Pathways of litter C by formation of aggregates and
751 SOM density fractions: Implications from ^{13}C natural abundance. Soil Biology
752 and Biochemistry 71, 95-104.

753 Guhra, T., Stolze, K., Totsche, K.U., 2021. Pathways of biogenically excreted organic
754 matter into soil aggregates, Soil Biology and Biochemistry 108483.
755 Https://doi.org/10.1016/j.soilbio.2021.108483.

756 Hamel, C., Hanson, K., Selles, F., Cruz, A.F., Lemke, R., McConkey, B., Zentner, R.,
757 2006. Seasonal and long-term resource-related variations in soil microbial
758 communities in wheat-based rotations of the Canadian prairie. Soil Biology and
759 Biochemistry 38, 2104–2116.

760 Hu, Y., Zheng, Q., Noll, L., Zhang, S., Wanek, W., 2020. Direct measurement of the
761 in situ decomposition of microbial-derived soil organic matter. Soil Biology and
762 Biochemistry 141, 107660.

763 Hu, Y., Zheng, Q., Wanek, W., 2017. Flux analysis of free amino sugars and amino
764 acids in soils by isotope tracing with a novel liquid chromatography/high

765 resolution mass spectrometry platform. Analytical Chemistry 89, 9192–9200.

766 Huang, Y., Liang, C., Duan, X., Chen, H., Li, D., 2019. Variation of microbial residue
767 contribution to soil organic carbon sequestration following land use change in a
768 subtropical karst region. Geoderma 353, 340-346.

769 Joergensen, R.G., 2018. Amino sugars as specific indices for fungal and bacterial
770 residues in soil. Biology and Fertility of Soils 54, 559-568.

771 Johnson, S.L., Kuske, C.R., Carney, T.D., Housman, D.C., Gallegos-Graves, L.V.,
772 Belnap, J., 2012. Increased temperature and altered summer precipitation have
773 differential effects on biological soil crusts in a dryland ecosystem. Global
774 Change Biology 18, 2583-2593.

775 Kaiser, C., Franklin, O., Dieckmann, U., Richter, A., 2014. Microbial community
776 dynamics alleviate stoichiometric constraints during litter decay. Ecology Letters
777 17, 680–690.

778 Khan, K.S., Mack, R., Castillo, X., Kaiser, M., Joergensen, R.G., 2016. Microbial
779 biomass, fungal and bacterial residues, and their relationships to the soil organic
780 matter C/N/P/S ratios. Geoderma 271, 115–123.

781 Koester M, Stock S, Nájera F, Abdallah K, Gorbushina A, Prietzel J, Matus F,
782 Klysubun W, Boy J, Kuzyakov Y, Dippold M, Spielvogel S 2021. From rock
783 eating to vegetarian ecosystems — disentangling processes of phosphorus
784 acquisition across biomes. Geoderma 388, 114827.

785 Kravchenko, A.N., Guber, A.K., Razavi, B.S., Koestel, J., Quigley, M.Y., Robertson,

786 G.P., Kuzyakov, Y., 2019. Microbial spatial footprint as a driver of soil carbon
787 stabilization. Nature Communications 10, 3121.

788 Krause, L., Biesgen, D., Treder, A., Schweizer, S.A., Klumpp, E., Knief, C., Siebers,
789 N., 2019. Initial microaggregate formation: Association of microorganisms to
790 montmorillonite-goethite aggregates under wetting and drying cycles. Geoderma
791 351, 250–260.

792 Kuzyakov, Y., Mason-Jones, K., 2018. Viruses in soil: Nano-scale undead drivers of
793 microbial life, biogeochemical turnover and ecosystem functions. Soil Biology
794 and Biochemistry 127, 305-317.

795 Kubiak-Ossowska, K., Tokarczyk, K., Jachimska, B., Mulheran, P.A., 2017. Bovine
796 Serum Albumin Adsorption at a Silica Surface Explored by Simulation and
797 Experiment. Journal of Physical Chemistry B 121, 3975–3986.

798 Lavallee, J.M., Soong, J.L., Cotrufo, M.F., 2019. Conceptualizing soil organic matter
799 into particulate and mineral- associated forms to address global change in the 21
800 st century. Global Change Biology 26, 261-273.

801 Legendre, P., Legendre, L., 2012. Numerical Ecology Ch 6 - Multidimensional
802 qualitative data. Developments in Environmental Modelling 24, 337–424.

803 Li, J., Cooper, J.M., Lin, Z., Li, Y., Yang, X., Zhao, B., 2015. Soil microbial
804 community structure and function are significantly affected by long-term organic
805 and mineral fertilization regimes in the North China Plain. Applied Soil Ecology
806 96, 75–87.

807 Li, J.Y., Jin, X.Y., Zhang, X.C., Chen, L., Liu, J.L., Zhang, H.M., Zhang, X., Zhang,
808 Y.F., Zhao, J.H., Ma, Z.S., Jin, D., 2020. Comparative metagenomics of two
809 distinct biological soil crusts in the Tengger Desert, China. Soil Biology and
810 Biochemistry 140, 107637.

811 Li, L., Wilson, C.B., He, H., Zhang, X., Zhou, F., Schaeffer, S.M., 2019. Physical,
812 biochemical, and microbial controls on amino sugar accumulation in soils under
813 long-term cover cropping and no-tillage farming. Soil Biology and Biochemistry
814 135, 369-378.

815 Li, Y., Nie, C., Liu, Y., Du, W., He, P., 2019. Soil microbial community composition
816 closely associates with specific enzyme activities and soil carbon chemistry in a
817 long-term nitrogen fertilized grassland. Science of the Total Environment 654,
818 264-274.

819 Liang, C., Amelung, W., Lehmann, J., Kästner, M., 2019. Quantitative assessment of
820 microbial necromass contribution to soil organic matter. Global Change Biology
821 25, 3578-3590.

822 Liang, C., Kästner, M., Joergensen, R.G., 2020. Microbial necromass on the rise: The
823 growing focus on its role in soil organic matter development. Soil Biology and
824 Biochemistry 150, 108000.

825 Liang, C., 2020. Soil microbial carbon pump: Mechanism and appraisal. Soil Ecology
826 Letters 2, 241–254.

827 Liang, C., Schimel, J.P., Jastrow, J.D., 2017. The importance of anabolism in

828 microbial control over soil carbon storage. Nature Microbiology 2, 17105.

829 Liu, Y., Zhao, L., Wang, Z., Liu, L., Zhang, P., Sun, J., Wang, B., Song, G., Li, X.,
830 2018. Changes in functional gene structure and metabolic potential of the
831 microbial community in biological soil crusts along a revegetation
832 chronosequence in the Tengger Desert. Soil Biology and Biochemistry 126, 40–
833 48.

834 Liu, Z., Sun, Y., Zhang, Y., Feng, W., Lai, Z., Fa, K., Qin, S., 2018. Metagenomic
835 and13C tracing evidence for autotrophic atmospheric carbon absorption in a
836 semiarid desert. Soil Biology and Biochemistry 125, 156–166.

837 López-Mondéjar, R., Brabcová, V., Štursová, M., Davidová, A., Jansa, J., Cajthaml,
838 T., Baldrian, P., 2018. Decomposer food web in a deciduous forest shows high
839 share of generalist microorganisms and importance of microbial biomass
840 recycling. ISME Journal 12, 1768-1778.

841 López-Mondéjar, R., Tláskal, V., Větrovský, T., Štursová, M., Toscan, R., Nunes, U.,
842 Baldrian, P., 2020. Metagenomics and stable isotope probing reveal the
843 complementary contribution of fungal and bacterial communities in the recycling
844 of dead biomass in forest soil. Soil Biology and Biochemistry 148, 107875.

845 Makino, W., Cotner, J.B., Sterner, R.W., Elser, J.J., 2003. Are bacteria more like
846 plants or animals? Growth rate and resource dependence of bacterial C:N:P
847 stoichiometry. Functional Ecology 17, 121-130.

848 Manzoni, S., Schimel, J.P., Porporato, A., 2012. Responses of soil microbial

communities to water stress: Results from a meta-analysis. Ecology 93, 930–938.

Matus, FJ 2021. Fine silt and clay content is the main factor defining maximal C and N accumulations in soils: a meta-analysis. Scientific Reports 11, 6438.

Miltner, A., Bombach, P., Schmidt-Brücken, B., Kästner, M., 2012. SOM genesis: Microbial biomass as a significant source. Biogeochemistry 111, 41–55.

Moorhead, D.L., Sinsabaugh, R.L., Hill, B.H., Weintraub, M.N., 2016. Vector analysis of ecoenzyme activities reveal constraints on coupled C, N and P dynamics. Soil Biology and Biochemistry 93, 1-7.

Mooshammer, M., Wanek, W., Zechmeister-Boltenstern, S., Richter, A., 2014. Stoichiometric imbalances between terrestrial decomposer communities and their resources: Mechanisms and implications of microbial adaptations to their resources. Frontiers in Microbiology 5, 22.

Persson, J., Fink, P., Goto, A., Hood, J.M., Jonas, J., Kato, S., 2010. To be or not to be what you eat: Regulation of stoichiometric homeostasis among autotrophs and heterotrophs. Oikos 119, 741–751.

Poeplau, C., Don, A., Six, J., Kaiser, M., Benbi, D., Chenu, C., Cotrufo, M.F., Derrien, D., Gioacchini, P., Grand, S., Gregorich, E., Griepentrog, M., Gunina, A., Haddix, M., Kuzyakov, Y., Kühnel, A., Macdonald, L.M., Soong, J., Trigalet, S., Vermeire, M.L., Rovira, P., van Wesemael, B., Wiesmeier, M., Yeasmin, S., Yevdokimov, I., Nieder, R., 2018. Isolating organic carbon fractions with varying turnover rates in temperate agricultural soils – A comprehensive method

comparison. Soil Biology and Biochemistry 125, 10-26.

Pointing, S.B., Belnap, J., 2012. Microbial colonization and controls in dryland systems. Nature Reviews Microbiology 10, 654.

Possinger, A.R., Zachman, M.J., Enders, A., Levin, B.D.A., Muller, D.A., Kourkoutis, L.F., Lehmann, J., 2020. Organo–organic and organo–mineral interfaces in soil at the nanometer scale. Nature Communications 11, 6103.

Prommer, J., Walker, T.W.N., Wanek, W., Braun, J., Zezula, D., Hu, Y., Hofhansl, F., Richter, A., 2019. Increased microbial growth, biomass, and turnover drive soil organic carbon accumulation at higher plant diversity. Global Change Biology 26, 669-681.

Rodriguez-Caballero, E., Belnap, J., Büdel, B., Crutzen, P.J., Andreae, M.O., Pöschl, U., Weber, B., 2018. Dryland photoautotrophic soil surface communities endangered by global change. Nature Geoscience 11, 185–189.

Samson, M.-élise, Chantigny, M.H., Vanasse, A., Menasseri-aubry, S., Royer, I., Angers, D.A., 2020. Management practices differently affect particulate and mineral-associated organic matter and their precursors in arable soils. Soil Biology and Biochemistry 148, 107867.

Samson, M.É., Chantigny, M.H., Vanasse, A., Menasseri-Aubry, S., Angers, D.A., 2020. Coarse mineral-associated organic matter is a pivotal fraction for SOM formation and is sensitive to the quality of organic inputs. Soil Biology and Biochemistry 149, 107935.

Schweigert, M., Herrmann, S., Miltner, A., Fester, T., Kästner, M., 2015. Fate of ectomycorrhizal fungal biomass in a soil bioreactor system and its contribution to soil organic matter formation. Soil Biology and Biochemistry 88, 120-127.

Shahbaz, M., Kuzyakov, Y., Sanaullah, M., Heitkamp, F., Zelenev, V., Kumar, A., Blagodatskaya, E., 2017. Microbial decomposition of soil organic matter is mediated by quality and quantity of crop residues: mechanisms and thresholds. Biology and Fertility of Soils 53, 287-301.

Shao, P., Lynch, L., Xie, H., Bao, X., Liang, C., 2021. Tradeoffs among microbial life history strategies influence the fate of microbial residues in subtropical forest soils. Soil Biology and Biochemistry 153, 108112.

Sokol, N.W., Bradford, M.A., 2018. Microbial formation of stable soil carbon is more efficient from belowground than aboveground input. Nature Geoscience 12, 46-53.

Sokol, N.W., Kuebbing, S.E., Karlsen-Ayala, E., Bradford, M.A., 2019. Evidence for the primacy of living root inputs, not root or shoot litter, in forming soil organic carbon. New Phytologist 221, 233-246.

Steven, B., Gallegos-Graves, L.V., Yeager, C.M., Belnap, J., Evans, R.D., Kuske, C.R., 2012. Dryland biological soil crust cyanobacteria show unexpected decreases in abundance under long-term elevated CO_2. Environmental Microbiology 14, 3247-3258.

Vance, E.D., Brookes, P.C., Jenkinson, D.S., 1987. An extraction method for

912 measuring soil microbial biomass C. Soil Biology and Biochemistry 19, 703–
913 707.

914 Wang B; An SS; Chao L; Liu Y; Kuzyakov Y 2021a. Microbial necromass as a
915 source of organic carbon in global ecosystems. Soil Biology and Biochemistry
916 162, 108422.

917 Wang, B., Liang, C., Yao, H., Yang, E., An, S., 2021b. The accumulation of microbial
918 necromass carbon from litter to mineral soil and its contribution to soil organic
919 carbon sequestration. Catena 207, 105622.

920 Walker, T.S., Bais, H.P., Grotewold, E., Vivanco, J.M., 2003. Update on Root
921 Exudation and Rhizosphere Biology Root Exudation and Rhizosphere Biology 1
922 132, 44–51.

923 Walkley, A., Black, I.A., 1934. An examination of the Degtjareff method for
924 determining soil organic matter, and proposed modification of the chromic acid
925 titration method. Soil Science 37, 29–38.

926 Warren, C., 2021. What are the products of enzymatic cleavage of organic N? Soil
927 Biology and Biochemistry 154, 108152.

928 Wu, J., Joergensen, R.G., Pommerening, B., Chaussod, R., Brookes, P.C., 1990.
929 Measurement of soil microbial biomass C by fumigation-extraction-an
930 automated procedure. Soil Biology and Biochemistry 22, 1167–1169.

931 Xia, Y., Chen, X., Zheng, X., Deng, S., Hu, Y., Zheng, S., He, X., Wu, J., kuzyakov,
932 Y., Su, Y., 2020. Preferential uptake of hydrophilic and hydrophobic compounds

933 by bacteria and fungi in upland and paddy soils. Soil Biology and Biochemistry
934 148, 107879.

935 Xu, H., Zhang, Y., Shao, X., Liu, N., 2022. Soil nitrogen and climate drive the
936 positive effect of biological soil crusts on soil organic carbon sequestration in
937 drylands: A Meta-analysis. Science of the Total Environment 803, 150030.

938 Yang, J.Q., Zhang, X., Bourg, I.C., Stone, H.A., 2021. 4D imaging reveals
939 mechanisms of clay-carbon protection and release. Nature Communications 12,
940 622.

941 Yao, X., Bowker, M.A., Xiao, B., 2020. Estimation of annual CO_2 efflux of moss
942 biocrust through measuring and simulating its respiration rate in a semiarid
943 climate. Geoderma 376, 114560.

944 Ye, G., Lin, Y., Kuzyakov, Y., Liu, D., Luo, J., Lindsey, S., Wang, W., Fan, J., Ding,
945 W., 2019. Manure over crop residues increases soil organic matter but decreases
946 microbial necromass relative contribution in upland Ultisols: Results of a 27-year
947 field experiment. Soil Biology and Biochemistry 134, 15-24.

948 Zechmeister-Boltenstern, S., Keiblinger, K.M., Mooshammer, M., Peñuelas, J.,
949 Richter, A., Sardans, J., Wanek, W., 2015. The application of ecological
950 stoichiometry to plant-microbial-soil organic matter transformations. Ecological
951 Monographs 85, 133-155.

952 Zhang, X., Amelung, W., 1996. Gas chromatograph1c determination of muramic acid,
953 glucosamine, mannosamine, and galactosamine in soils. Soil Biology and

954 Biochemistry 28, 1201–1206.

955 Zhang, X., Jia, J., Chen, L., Chu, H., He, J.S., Zhang, Y., Feng, X., 2021. Aridity and
956 NPP constrain contribution of microbial necromass to soil organic carbon in the
957 Qinghai-Tibet alpine grasslands. Soil Biology and Biochemistry 156, 108213.

Figure legends:

Fig. 1. Dynamics of fungal necromass carbon (C) and bacterial necromass C, fungal:bacterial necromass ratio, microbial necromass C contribution to soil organic C, fungal and bacterial necromass C contribution to soil organic C, fungal necromass to total microbial necromass C ratio, necromass accumulation coefficient (microbial necromass C/living microbial biomass C: necromass accumulation per unit of microbial biomass C) in biological soil crusts (BSC) horizon and in the 0–2 cm of BSC-underlying mineral soil during 5 stages of BSC formation: bare sand (~ 0–1 years old), cyanobacteria stage (Cy, ~ 3–7 years old), cyanobacteria-moss stage (Cy-Mo, ~ 8–13 years old), moss-cyanobacteria stage (Mo-Cy, ~ 20–25 years old), and moss stage (Mo, ~ 30 years old). Total microbial necromass C was estimated as the sum of fungal and bacterial necromass C. Values are presented as the means of 5 replicates ± standard error (SE). Lowercase and uppercase letters indicate significant differences between the biological soil crust stages ($p < 0.05$). SOC, soil organic carbon; MNC, microbial necromass carbon.

Fig. 2. Activities of β-1,4-glucosidase (BG), β-1,4-N-acetyl-glucosaminidase (NAG), leucine aminopeptidase (LAP) and alkaline phosphatase (AP), C- and N- acquiring enzyme activity/microbial biomass C (MBC)- and N (MBN)- ratio (specific enzyme activity per microbial biomass unit: microbial enzyme activity coefficient) in the biological soil crust (BSC) horizon and in the 0–2 cm of BSC-underlying mineral soil during 5 stages of BSC formation: bare sand, cyanobacteria stage (Cy),

cyanobacteria-moss stage (Cy-Mo), moss-cyanobacteria stage (Mo-Cy), and moss stage (Mo). Values are presented as the means of 5 replicates ± standard error (SE). Letters indicate significant differences between the biological soil crust stages ($p < 0.05$).

Fig. 3. Top: Vector length and angle of enzymatic stoichiometry in the BSC horizon and 0–2 cm soil reflecting the microbial C and N limitations during biocrust formation (5 stages): bare sand, cyanobacteria stage (Cy), cyanobacteria-moss stage (Cy-Mo), moss-cyanobacteria stage (Mo-Cy), and moss stage (Mo). Values are the means of 5 replicates ± standard error (SE). Lowercase and uppercase letters indicate significant differences in BSC and 0–2 cm between the biological soil crust stages, respectively. A vector angle of < 45° denotes N limitation (red horizontal dashed line), and angles > 45° denote P limitation. **Bottom:** Stoichiometric analysis of soil enzyme activities to identify the C, N and P limitations in soil. By using 1.0 as a horizontal and vertical baseline along the axes of enzyme activity ratios (NAG+LAP/AP as x-axis and BG/NAG+LAP as y-axis), four groups of microbial resource limitations were categorized: N limitation, P limitation, C and N colimitation, and C and P colimitation. Nearly all stages (except Bare sand) and replicates are clearly N limited (light yellow shaded area).

Fig. 4. Regressions of soil organic C with particulate and mineral-associated organic C (POC and MAOC); soil organic C (SOC) a fungal, bacterial and microbial

1002 necromass C; mineral-associated organic C with fungal, bacterial and microbial
1003 necromass C; and particulate organic C with fungal, bacterial and microbial
1004 necromass C. All regression lines are significant at $p < 0.001$. BNC, bacterial
1005 necromass C; FNC, fungal necromass C; MNC, total microbial necromass C. The
1006 black dashed line indicates a 1:1 relationship.
1007
1008 **Fig. 5.** Regressions of microbial necromass C with particulate (POC) and
1009 mineral-associated organic C (MAOC), soil organic C (SOC) with the POC/MAOC
1010 ratio, and soil clay and silt content with bacterial and fungal necromass C. All
1011 regression lines are significant at $p < 0.05$. The black dashed line indicates a 1:1
1012 relationship.
1013
1014
1015 **Fig. 6.** Redundancy analysis (RDA) identifies the relationships between microbial
1016 biomass, extracellular enzyme activities, available nutrients, particulate organic C,
1017 mineral-associated organic C, clay content, and microbial necromass C. The red
1018 arrows indicate explanatory variables, and the black arrows indicate response
1019 variables. The points represent the stages of biocrust formation. The explanatory ratio
1020 we use in this study is the simple effect. The light red bars represent microbial
1021 biomass C, N, P content, the light green bars represent the four extracellular enzyme
1022 activities and the light blue bars represent other soil properties. BNC, bacterial
1023 necromass C; FNC, fungal necromass C; MNC, total microbial necromass C; GlcN,

1024 glucosamine; GalN, galactosamine; ManN, mannosamine; MurA, muramic acid; F/B
1025 necromass, fungal/bacterial necromass; DC, dissolved carbon; DN, dissolved nitrogen;
1026 DP, dissolved phosphorus; MBC, microbial biomass carbon; MBN, microbial biomass
1027 nitrogen; MBP, microbial biomass phosphorus; BG, β-1,4-glucosidase; NAG,
1028 β-1,4-N-acetyl-glucosaminidase; LAP, leucine aminopeptidase; AP, alkaline
1029 phosphatase; POC, particulate organic carbon; MAOC, mineral-associated organic
1030 carbon. *$p < 0.05$, **$p < 0.01$.
1031
1032 **Fig. 7.** Conceptual framework for the preservation, decomposition and stabilization of
1033 microbial necromass in biological crust dominated sandy soils. Microbial N demand
1034 (X axis) and clay conservation (Y axis) regulate microbial necromass decomposition
1035 and accumulation, further determining particulate organic carbon (POC) and
1036 mineral-associated organic carbon (MAOC) pool formation. Saturation of MAOC
1037 accumulation due to low clay content led to more microbial necromass being
1038 incorporated into the POC pool. However, the increase of soil clay content by
1039 weathering eliminates MAOC saturation during pedogenesis. MAOC did not always
1040 increase after saturation, but POC increased with the microbial necromass, suggesting
1041 that the limitation of MAOC increase by low clay content contributed more to POC
1042 than MAOC accumulation. The curved dotted arrow shows the accelerated POC
1043 compared to MAOC accumulation after the MAOC saturation. The N limitation of
1044 microorganisms and limited clay protection and MAOC saturation resulted in a lower
1045 necromass accumulation coefficient, which led to a much lower contribution of

microbial necromass to SOC in the initial formation of biocrust-covered sandy soil.

Table 1 The content of carbon (C), nitrogen (N), and phosphorus (P) contents in the bulk soil, microbial biomass and dissolved matter, amino sugar (glucosamine (GlcN), galactosamine (GalN), mannosamine (ManN) and muramic acid (MurA)), particulate organic carbon (POC) and mineral-associated organic carbon (MAOC) and the mass ratio of POC to MAOC, and soil clay (%), silt (%) and sand (%) contents in biological soil crusts (BSC) horizon and in the 0–2 cm of BSC-underlying mineral soil during 5 stages of BSC formation: bare sand (~ 0–1 years old), cyanobacteria stage (Cy, ~ 3–7 years old), cyanobacteria-moss stage (Cy-Mo, ~ 8–13 years old), moss-cyanobacteria stage (Mo-Cy, ~ 20–25 years old), and moss stage (Mo, ~ 30 years old). Values are the means of 5 replicates ± standard error (SE). Lowercase and uppercase letters indicate significant differences in BSC and the 0–2 cm soil horizons between the biological soil crust stages, respectively ($p < 0.05$).

	Bare sand	Cyanobacteria		Cyanobacteria-moss		Moss-cyanobacteria		Moss	
	0-2 cm	BSC	0-2 cm	BSC	0-2cm	BSC	0-2cm	BSC	0-2cm
SOC (g kg^{-1})	2.44±0.29B	15.2±3.08b	6.73±1.97A	17.8±3.20ab	5.45±1.24A	20.0±3.00a	6.00±2.00A	19.8±4.00a	6.14±2.76A
TN (g kg^{-1})	0.10±0.01B	1.10±0.27b	0.46±0.14A	1.14±0.26b	0.42±0.11A	1.38±0.16a	0.49±0.14A	1.30±0.26ab	0.46±0.19A
TP (g kg^{-1})	0.19±0.02B	0.40±0.02b	0.32±0.03A	0.40±0.04ab	0.32±0.04A	0.45±0.06a	0.34±0.05A	0.39±0.03ab	0.31±0.03A
MBC (mg kg^{-1})	12.3±6.44C	812±204b	143±60AB	957±233b	86±34B	2199±235a	177±54A	2174±475a	140±84AB
MBN (mg kg^{-1})	6.25±2.82C	259±44b	59±27AB	273±25b	52±18B	399±13a	79±18A	458±27a	71±26AB
MBP (mg kg^{-1})	4.57±2.25A	8.21±4.56b	3.83±2.02A	15.8±6.95b	4.78±2.59A	38.6±15.2a	5.13±2.56A	35.8±11.1a	5.72±3.83A
DC (mg kg^{-1})	9.18±1.01C	72.2±14.0b	46.4±24.0AB	79.3±16.8b	29.5±8.81B	128±42.9a	45.7±15.3A	139±51.0a	33.1±9.10AB
DN (mg kg^{-1})	8.84±2.99C	92.6±22.5a	25.5±7.26AB	115±27.1a	21.7±6.84B	108±12.0a	24.0±6.77AB	115±47.0a	30.6±12.9A
DP (mg kg^{-1})	9.24±4.3A	4.82±1.11b	6.10±1.33B	7.34±5.42b	6.66±4.23AB	11.9±1.26a	7.69±2.07AB	14.0±2.43a	9.38±1.27A
GlcN (mg kg^{-1})	29.6±3.23B	329±94a	159±31A	310±49a	127±28A	369±91a	151±57A	323±137a	147±96A

ManN (mg kg^{-1})	1.11±0.21B	12.6±4.61a	5.97±1.89A	13.8±2.73a	4.38±0.90A	13.85±3.89a	4.38±1.45A	10.2±1.78a	4.92±2.09A
GalN (mg kg^{-1})	12.1±2.19A	148±38a	85±8.8.78A	130±27a	71±18A	141±32a	66±24A	121±31a	61±31A
MurA (mg kg^{-1})	1.42±0.26C	26.6±9.77a	7.11±1.26A	27.9±7.62a	5.54±0.99B	30.4±4.28a	5.47±0.98B	24.4±5.40a	4.55±2.16B
POC (g kg^{-1})	0.63±0.15C	6.31±2.42b	3.16±0.88A	3.55±1.05b	1.68±0.41B	6.39±2.70b	1.41±0.57BC	9.47±3.21a	2.60±1.18A
MAOC (g kg^{-1})	1.67±0.34B	7.39±1.56b	3.17±0.63A	5..27±0.72c	2.44±0.49A	7.22±1.33b	2.65±0.46A	12.57±2.68a	2.90±1.15A
$POC_{Mass\ ratio}$	92.3%±0.60%A	68.9%±6.15%a	63.0%±5.90%B	62.6%±4.34%a	62.6%±4.34%B	65.8%±1.21%a	62.6%±2.05%B	61.3%±3.53%a	69.1%±5.50%B
$MAOC_{Mass\ ratio}$	7.72%±0.60%B	31.1%±6.15a	37.0%±5.90%A	37.4%±4.34%a	37.4%±4.34%A	34.2%±1.21%a	37.4%±2.05%A	38.7%±3.54%a	30.9%±5.50%A
Clay (%)	0.21%±0.08%	1.89%±0.45%	1.58%±0.67%	1.56%±0.35%	1.56%±0.66%	1.40%±0.46%	1.28%±0.43%	1.24%±0.45%	1.27%±0.56%
Silt (%)	6.84%±1.15%	47.4%±11.3%	37.3%±10.2%	41.1%±2.35%	38.1%±12.2%	38.3%±9.42%	37.5%±8.88%	33.9%±10.3%	31.5%±13.5%
Sand (%)	92.9%±1.20%	50.8%±11.7%	61.1%±10.8%	57.5%±2.72%	60.3%±9.87%	60.3%±9.87%	61.2%±9.14%	64.8%±10.8%	67.2%±14.1%

1054 **Supplementary Figures**

1055 **Fig. S1.** Relationships between fungal, bacterial, and microbial necromass and C, N,
1056 and P in microbial biomass and dissolved C, N and P and enzyme activities. Only the
1057 regression lines significant at $p < 0.05$ are presented. BG, β-1,4-glucosidase; NAG,
1058 β-1,4-N-acetyl-glucosaminidase; LAP, leucine aminopeptidase; AP, alkaline
1059 phosphatase. BNC, bacterial necromass C; FNC, fungal necromass C; MNC, total
1060 microbial necromass C.

1061

1062 **Fig. S2.** Relationships between the log of microbial biomass carbon/nitrogen (C/N)
1063 ratio and log of ratio of the C/N in bulk soil, dissolved matter and enzymes. Only the
1064 regression lines significant at $p < 0.05$ are presented. The coefficient 1/H is the slope
1065 of the regression between log (resource ratio, C/N in bulk soil, dissolved matter and
1066 enzyme) and log (biomass ratio, microbial biomass C/N), which represent the degree
1067 of microbial stoichiometric homeostasis. The regression relationship was
1068 nonsignificant ($p > 0.05$), 1/H was set to zero, and the microorganisms were
1069 considered "strictly homeostatic". Microorganisms maintain constant biomass C/N
1070 ratios regardless of the changes in C/N in bulk soil, dissolved matter and enzymes.

1071

1072 **Fig. S3.** Relationships of the log of fungal and bacterial necromass C, log of microbial
1073 biomass C/N and soil dissolved organic C/N. FNC, fungal necromass C; BNC,
1074 bacterial necromass C; MNC, microbial necromass C.

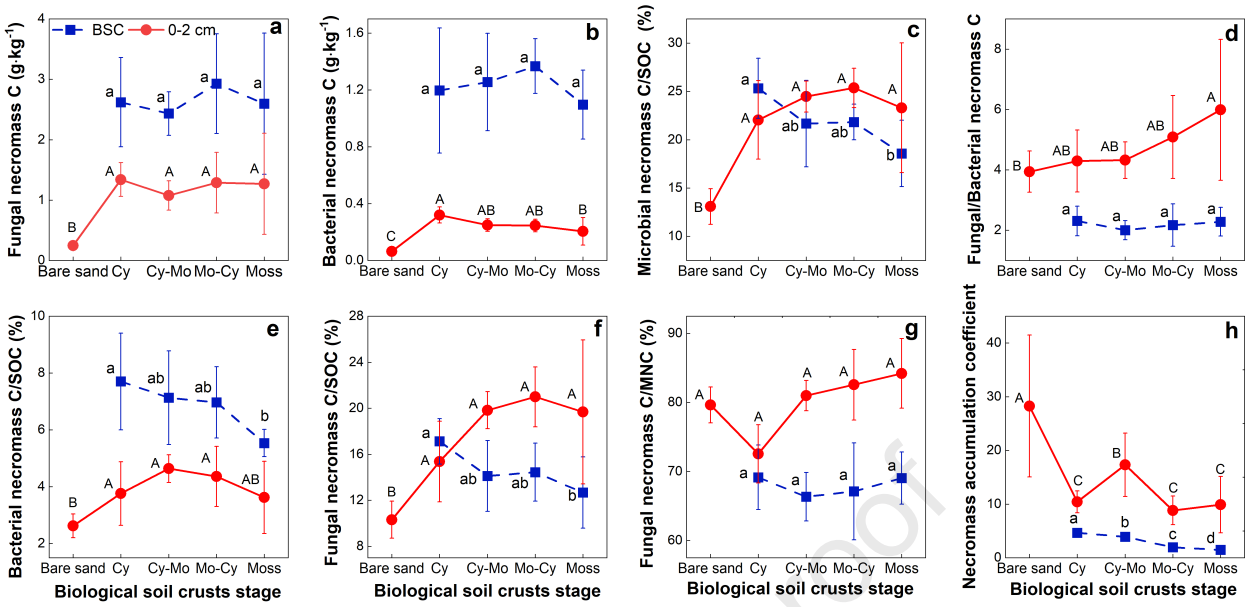

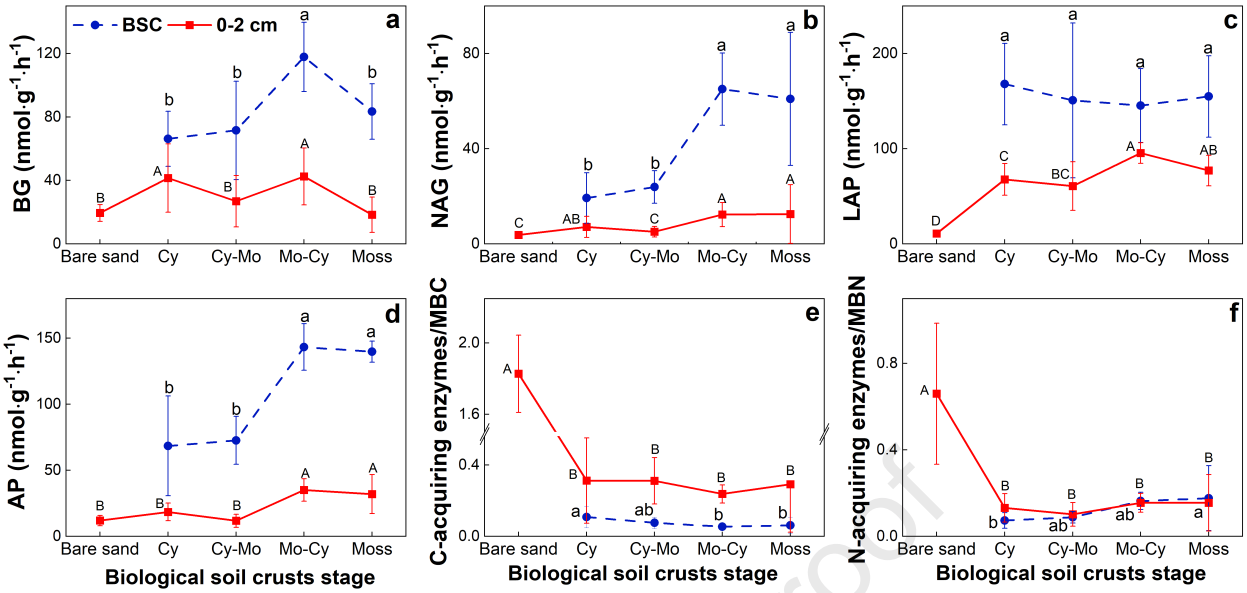

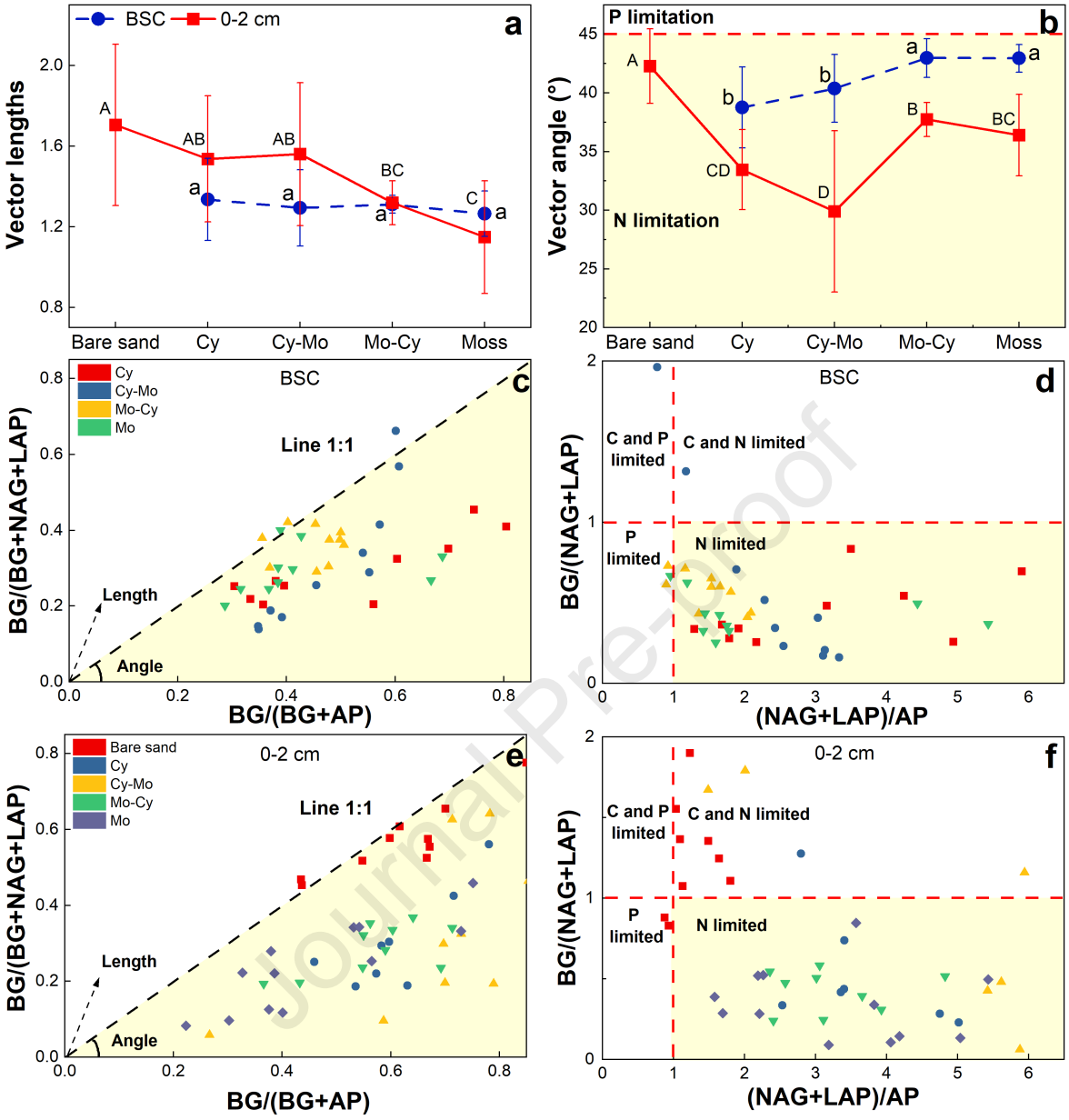

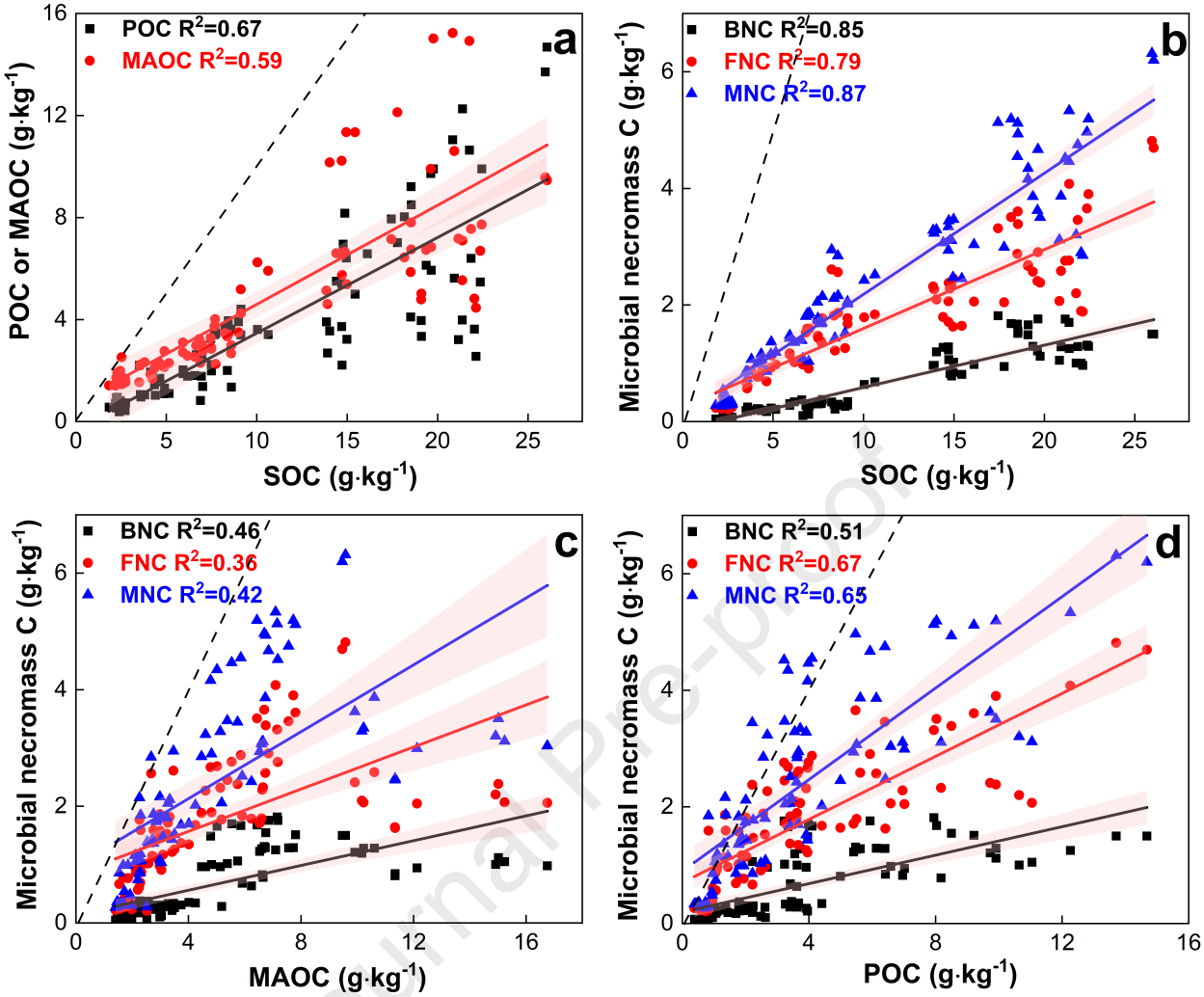

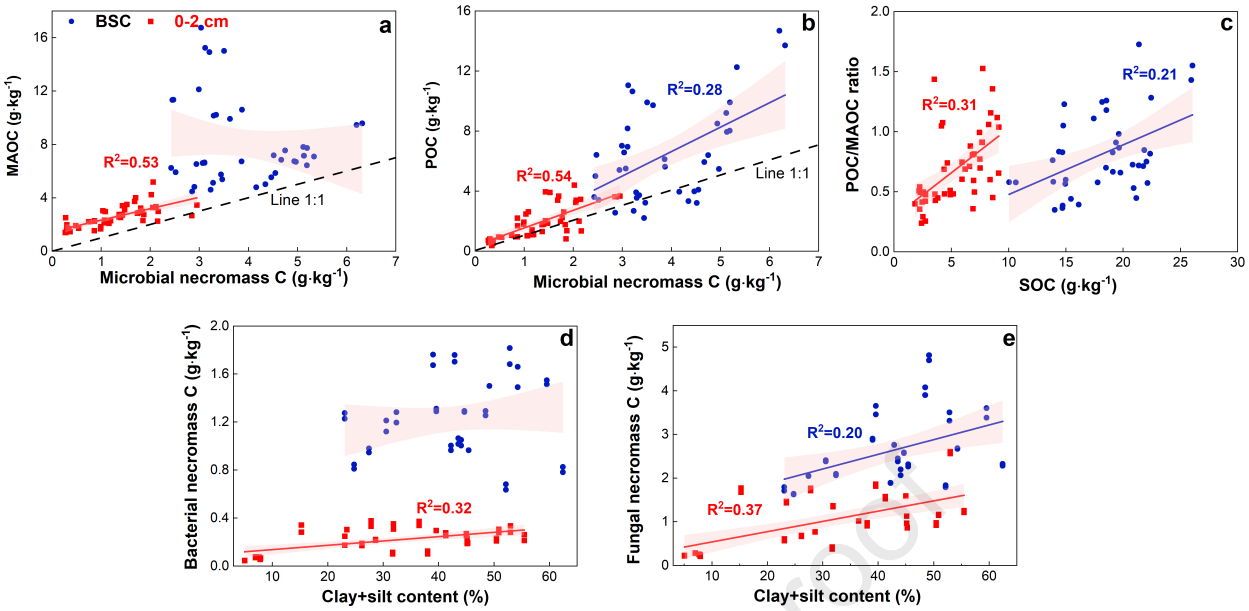

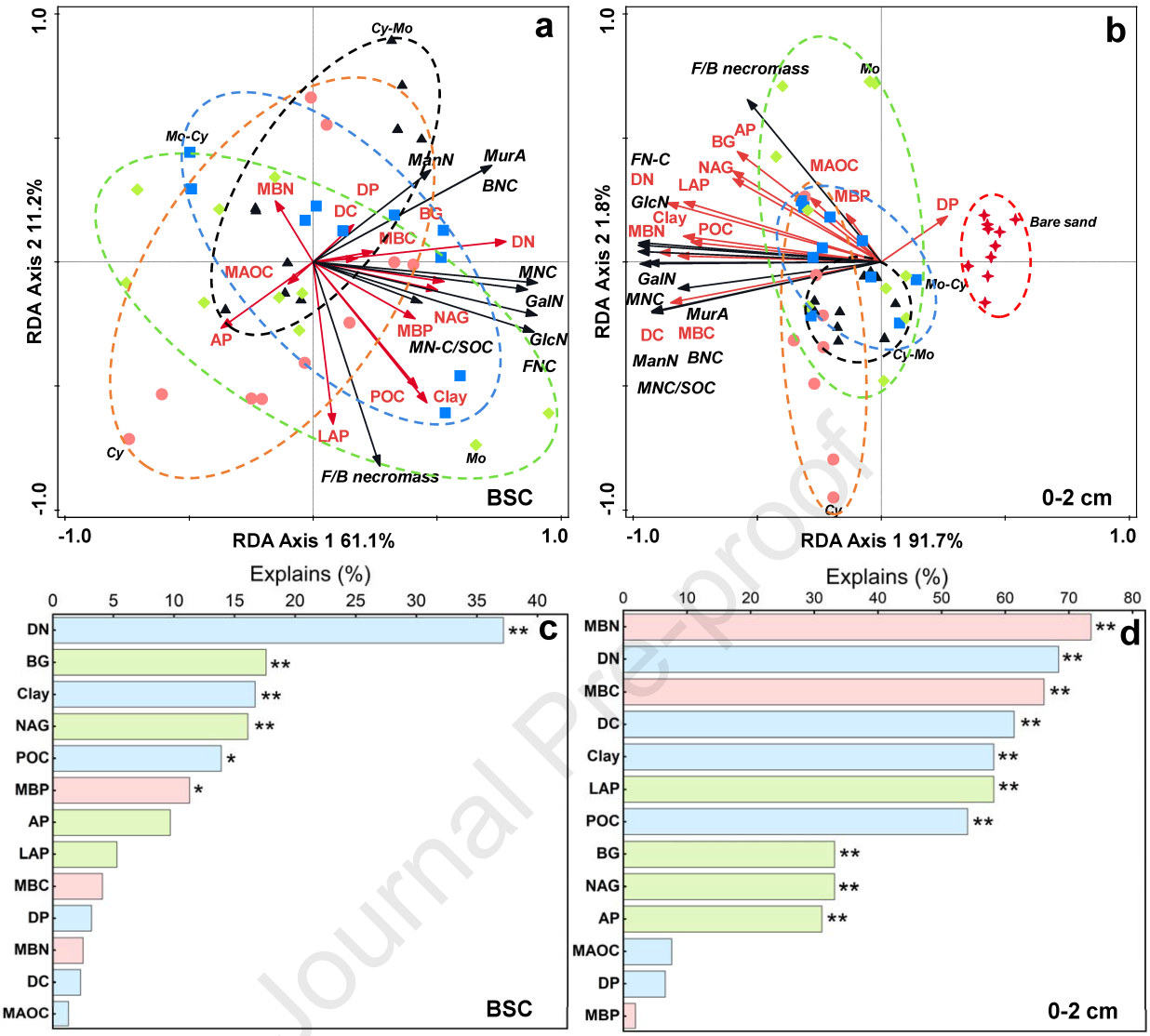

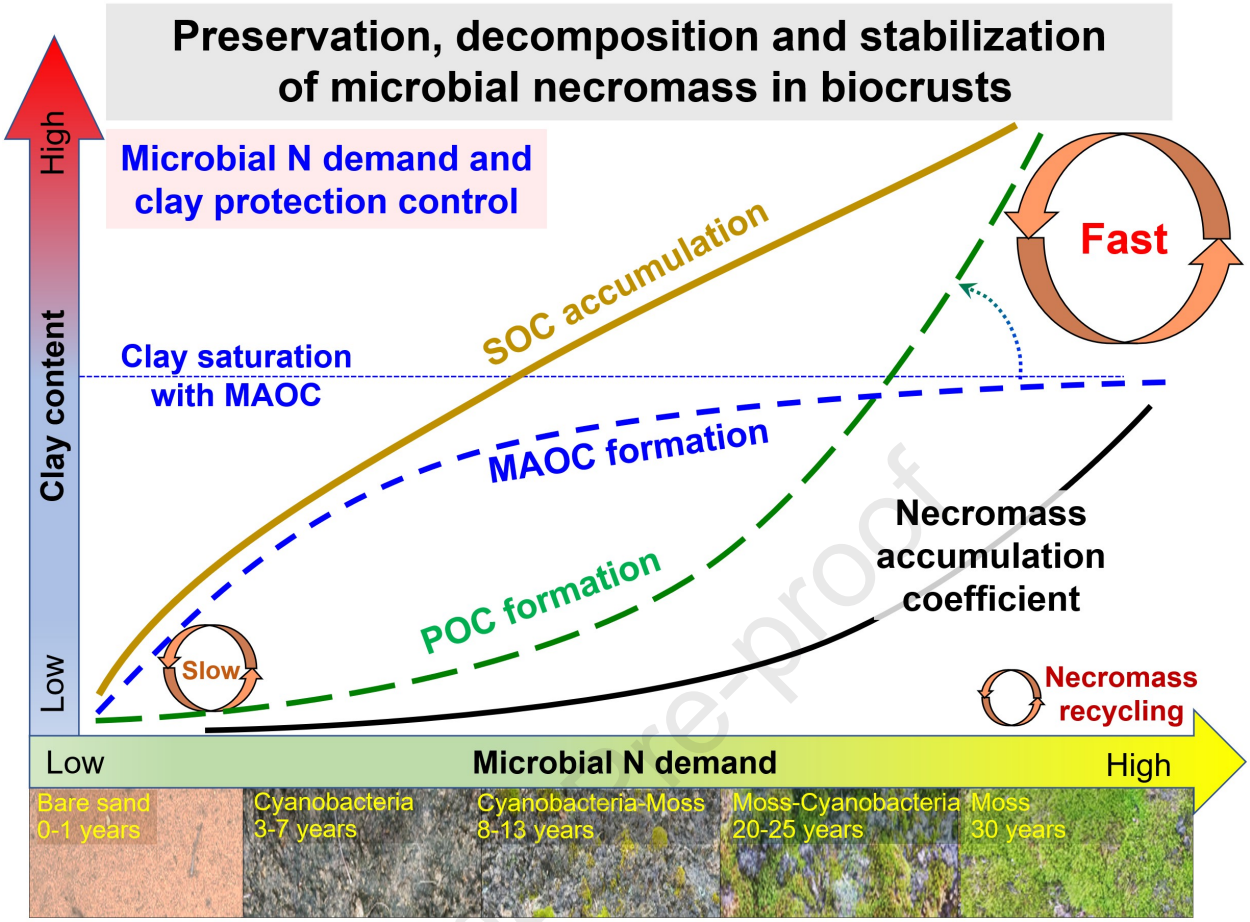

Highlights:

- Microbial necromass C contribution to SOC in biocrust-covered sandy soils was less than 25%
- Biocrust-covered sandy soils have a low necromass accumulation coefficient
- Low soil clay content leads to more microbial necromass forming particulate organic carbon
- Microbial nitrogen limitation was common in biocrust formation sequences
- Microbial N limitation and insufficient clay protection control the necromass dynamics

Declaration of interests

☒ **The authors declare that they have no known competing financial interests or personal relationships that could have appeared to influence the work reported in this paper.**

☐The authors declare the following financial interests/personal relationships which may be considered as potential competing interests: